



The contents of the three courses and the methods of application are on the ECMWF website at

<http://www.ecmwf.int/newsevents/training/2010>

- ◆ **Use and Interpretation of ECMWF Products.**
This is mainly aimed at forecasters or people with forecasting experience.
Deadline for applications: 11 December 2009.
- ◆ **Use of computing facilities.**
There are six modules aimed at both current and potential users of the Centre's facilities.
Deadline for applications: 11 December 2009.
- ◆ **Numerical Weather Prediction.**
There are four modules providing scientific training on a variety of topics including numerical methods, parametrization of physical processes, data assimilation and predictability.
Deadline for applications: 26 February 2010.

The dates of the courses/modules are given on page 34 of this newsletter.

Contents

Editorial 1

News

New items on the ECMWF website 2
 Co-operation agreement with Bulgaria 2
 Changes to the operational forecasting system 3
 Results of the readership survey 3
 Operational assimilation of NOAA-19 ATOVS data 4
 Thirty years of world-class weather forecasts 6

Meteorology

The new all-sky assimilation system for
 passive microwave satellite imager observations 7
 Tracking fronts and extra-tropical cyclones 9
 Progress in the implementation of Hydrological
 Ensemble Prediction Systems (HEPS) in Europe
 for operational flood forecasting 20
 An experiment with a 46-day
 Ensemble Prediction System 25
 Evaluation of AMVs derived from
 ECMWF model simulations 30

General

ECMWF Calendar 2010 34
 ECMWF publications 34
 Index of past newsletter articles 35
 Useful names and telephone numbers
 within ECMWF inside back cover

Publication policy

The *ECMWF Newsletter* is published quarterly. Its purpose is to make users of ECMWF products, collaborators with ECMWF and the wider meteorological community aware of new developments at ECMWF and the use that can be made of ECMWF products. Most articles are prepared by staff at ECMWF, but articles are also welcome from people working elsewhere, especially those from Member States and Co-operating States. The *ECMWF Newsletter* is not peer-reviewed.

Editor: Bob Riddaway

Typesetting and Graphics: Rob Hine

Any queries about the content or distribution of the *ECMWF Newsletter* should be sent to Bob.Riddaway@ecmwf.int

Guidance about submitting an article is available at www.ecmwf.int/publications/newsletter/guidance.pdf

Contacting ECMWF

Shinfield Park, Reading, Berkshire RG2 9AX, UK

Fax:+44 118 986 9450

Telephone: National0118 949 9000

International+44 118 949 9000

ECMWF website<http://www.ecmwf.int>

A “green” ECMWF

Since the beginning of its operations ECMWF has paid very serious attention to having an energy-efficient infrastructure. This was initially driven by cost-efficiency considerations. In recent years, however, this concern has become a dominant issue for two main reasons.

The rise and volatility of electricity prices resulted in this becoming a major issue. The cost of electricity not only accounts for about 7% of the Centre's budget, but is also one of the main financial risks.

ECMWF and its Member States are paying a lot of attention to their impact on carbon emissions. Operating in the field of atmospheric sciences, which has provided the basic insights that have alerted the world to the global warming issue, makes us especially aware of these considerations and raises expectations others have of ECMWF.

Therefore ECMWF must be exemplary in terms of energy-efficiency and strive to have a carbon footprint that is as low as possible for its infrastructure. This requires improving all related aspects of ECMWF's services and facilities.

For obvious reasons, the main area of action has to be the high-performance computing services which account for about 95% of ECMWF's energy consumption, now 4 MW. During the recent supercomputer procurement, energy efficiency was a main selection criteria. On a 'FLOPS/kW' rating, the Centre's new supercomputer is about twice as efficient as the system it replaces and the next phase expected in 2011 will further improve this ratio by a factor of about 4. Also the recently installed cooling equipment is much more energy-efficient than the previous devices. However, as our mission requires a steady increase in computing performance, it is necessary to look at all possible ways of improving energy efficiency. This includes consideration of cooling technologies, power distribution, power generation and data centre design.

On all these issues ECMWF is working in close cooperation with its Member States. A meeting addressing these issues was held at ECMWF on 7 October, where there were some presentations about recent experience in improving energy efficiency. Also a subgroup of the Technical Advisory Committee has been established that will review the whole issue of 'green computing' and allow experience-sharing. As ECMWF's infrastructure is now quite old and predates emerging considerations on energy-efficiency, it restricts the options that could otherwise be open. Therefore relocating the data centre to somewhere more suitable, such as close to a power source, near a source of free cooling or where waste heat can be used, will need to be investigated.

Other areas must also be considered with the aim of reducing our carbon footprint and other environmental impacts, such as water usage and general waste reduction, wherever practicable. Our goal is that ECMWF should not only be a leader in global Numerical Weather Prediction, but also do it whilst being an exemplary 'green' institution.

Dominique Marbouty

New items on the ECMWF website

ANDY BRADY

Forecasting system horizontal resolution increase

In autumn 2009, ECMWF is planning to upgrade the horizontal resolution of its deterministic forecasting system and the Ensemble Prediction System (EPS), including the monthly extension, to 32 days. The schedule for implementation of these changes is available but is subject to change.

- http://www.ecmwf.int/products/changes/horizontal_resolution_2009/

New GRIB-2 high resolution products

The Council, at its 70th session (December 2008), agreed to make the GTS data sets available to NHMSs of WMO members at a spatial resolution of 0.5° latitude/longitude. These data sets have been made available in GRIB-2 via ftp from ECMWF's data server.

- <http://www.ecmwf.int/products/additional/>

Early access to GRIB edition 2

ECMWF will implement the use of GRIB edition 2 in its operational forecasting system with the next increase of the vertical resolution, which is planned for mid-2010. Dissemination of model level data encoded in GRIB edition 1 will cease at the time of this implementation. Users of the Centre's model level data are therefore invited to test their software with products encoded in GRIB edition 2 as soon as possible.

- <http://www.ecmwf.int/services/dissemination/grib2test.html>

Metview

A new export version of Metview (3.11.5-export) was made available to users on 7 September 2009. Documentation of this update is available on the Metview pages. Metview capabilities include powerful data access, processing and visualisation.

- <http://www.ecmwf.int/publications/manuals/metview/>

The ECMWF Seminar 2009

Every year ECMWF organizes a seminar with a pedagogical objective, whereby a selected topic related to numerical weather prediction is highlighted. The subject of the seminar this year was '*Seminar on Diagnosis of Forecasting and Data Assimilation Systems*'. The seminar this year ran from 7 to 10 September 2009.

- http://www.ecmwf.int/newsevents/meetings/annual_seminar/2009/

Information leaflets

A selection of information leaflets about ECMWF and its main activities is now available. The leaflets are available in English, French and German. They outline the history of ECMWF and ECMWF's involvements in climate research, GEMS (Global and Regional Earth System Monitoring with Satellite and In-situ Data), severe weather and ocean waves.

- http://www.ecmwf.int/about/information_leaflets/

Co-operation agreement with Bulgaria

MANFRED KLÖPPEL

On 22 July 2009, Prof Nikola Sabotinov, President of the Bulgarian Academy of Science, and Mr Dominique Marbouty, Director of ECMWF, signed a co-operation agreement at ECMWF's headquarters in Reading. Prof Konstantin Tsankov, General Director of the National Institute of Meteorology and Hydrology, and Mr Plamen Dimitrov, Minister Plenipotentiary, Bulgarian Embassy in London, attended the ceremony.

Prof Sabotinov stated: "I take great pleasure in signing this co-operation agreement with the European Centre for Medium-Range Weather Forecasts, the world leader in numerical weather prediction. Being a Member State of the European Union since 2007, it is essential for Bulgaria to also have closer links to European centres of



excellence, such as ECMWF. The information we receive from ECMWF will be a great help to Bulgarian institutions as they strive to deliver

Signing the co-operation agreement. Dominique Marbouty, Nikola Sabotinov and Konstantin Tsankov (left to right) signing the agreement for Bulgaria to become a Co-operating State.

top quality services to the general public. I am confident that in particular the National Institute of Meteorology and Hydrology will benefit immensely from this close co-operation.”

Prof Tzankov said: “This co-operation agreement is highly significant for the Bulgarian National Institute of Meteorology and Hydrology. I am confident that closer collaboration with ECMWF will enable us to issue earlier advice on the likelihood of extreme weather, such as the storms and heavy precipitation we experienced in the past years. We will be able to pass on the information we receive as a Co-operating State to both the public and the authorities responsible so that they can prepare for and respond to adverse weather

events more effectively. We welcome the opportunity to share knowledge and expertise with our colleagues at ECMWF and will use ECMWF’s products to improve our forecasts and extend their range. We very much value this agreement and the benefits it will bring to the people of Bulgaria.”

Mr Marbouty said: “ECMWF owes its reputation as world leader in the field of numerical weather prediction to close collaboration with the meteorological community worldwide, and particularly in Europe. Governments are becoming increasingly aware of the need to improve the quality and accuracy of numerical weather prediction in order to obtain advance warning of severe weather events such as storms, heat waves and floods. I look forward to working closely with

the Bulgarian National Institute of Meteorology and Hydrology and am pleased to offer the agency access to all our products, especially medium-range weather forecasts.”

Bulgaria will become ECMWF’s fourteenth Co-operating State. Co-operation agreements offer full access to ECMWF real-time products, archive data and software tools, as well as access to ECMWF training facilities. The agreement will allow Bulgaria to become a full ECMWF Member State in the near future.

To date, Co-operation Agreements have been signed with the following countries: Bulgaria, Croatia, Czech Republic, Estonia, Iceland, Hungary, Latvia, Lithuania, Montenegro, Morocco, Romania, Serbia, Slovakia and Slovenia.

Changes to the operational forecasting system

DAVID RICHARDSON

New cycle (Cy35r3)

A new cycle of the ECMWF forecast and analysis system, Cy35r3, was introduced into operations on 8 September 2009. Changes for this cycle include:

- Assimilation of cloud-affected radiances for infra-red instruments.
- Improved assimilation of satellite channels that are sensitive to the land surface.
- Assimilation of total column water vapour data from the MERIS instrument onboard ENVISAT .

- Variational bias correction for ozone satellite data.
- Improved quality control (using Huber norm) of conventional observations.
- Improved background-error statistics for humidity, new humidity formulation in 4D-Var.
- Weak-constraint 4D-Var taking into account systematic model errors in the stratosphere.
- Non-orographic gravity wave scheme.
- New trace gas climatology.
- Further revision of the snow scheme.

- Revised stochastic physics (model perturbations) for EPS.

Overall, there is a clear improvement over the northern hemisphere; the change is neutral for the southern hemisphere. The non-orographic gravity wave scheme improves the stratospheric circulation. The main impact of the EPS change is to improve the probabilistic performance for temperature in the tropics.

Information about the evolution of the operational forecasting system can be found at:

- <http://www.ecmwf.int/products/changes/>

Results of the readership survey

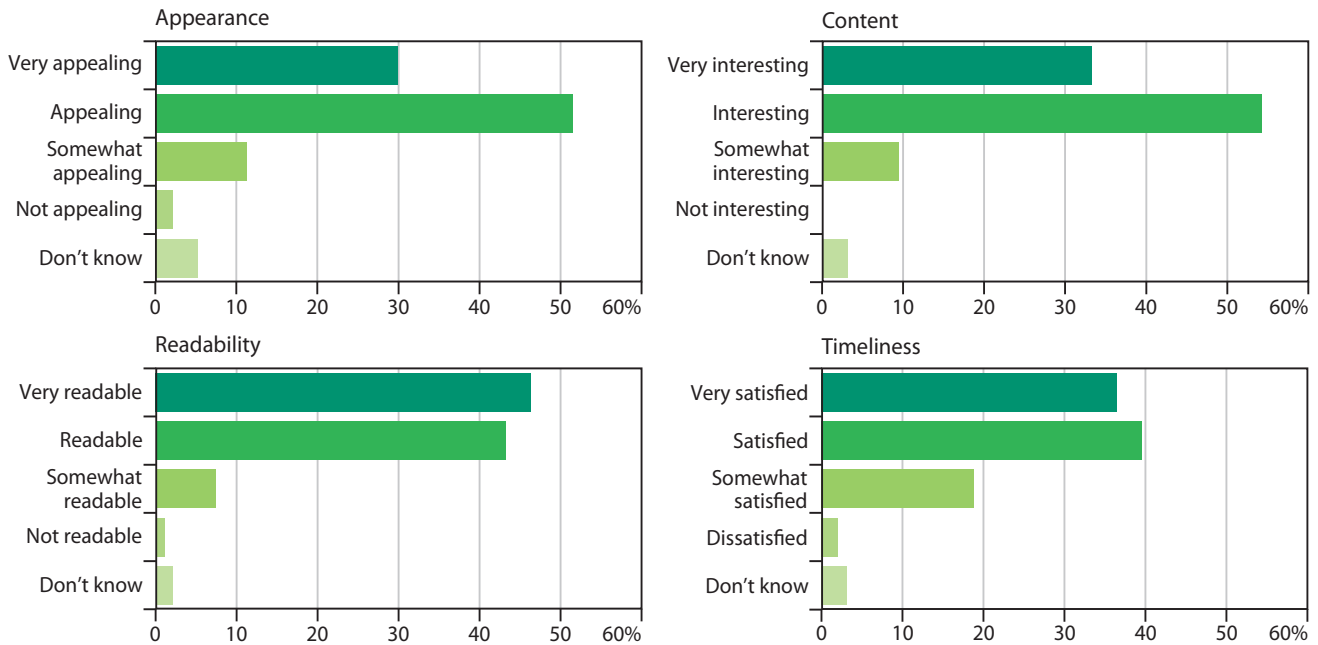
BOB RIDDAWAY

The views of readers of the *ECMWF Newsletter* were sought via a questionnaire accessible from the ECMWF website from April to July 2009. It appears that there is a high level of satisfaction with the appearance, content, readability and timeliness of the newsletter, though efforts will continue to be made to improve these aspects.

Indeed, some changes have been introduced into this edition.

With regard to the importance of the various types of items in the newsletter, readers were asked to assess them according to whether they are ‘very important’, ‘important’, ‘somewhat important’, ‘not important’ and ‘don’t know’. The following are the combined scores for the ‘very important’ and ‘important’ responses.

- Editorial: 71.1%.
- Changes to the forecasting system: 86.2%.
- New items on the ECMWF website: 79.3%.
- Other news items: 66.7%.
- Meteorological articles: 92.5%.
- Computing articles: 60.0%.
- Calendar: 60.0%.
- ECMWF publications: 69.8%.
- Index of past articles: 57.6%.



Some results from the readership survey. The results are shown for the level of satisfaction with the appearance, content, readability and timeliness of items in the ECMWF Newsletter. Overall there is a high level of satisfaction. The results are based on 96 responses.

Clearly the meteorological articles are those of most interest to readers, with the changes to the forecasting system, new items on the ECMWF website and editorial also having particularly high levels of interest.

There were many interesting suggestions about how to improve the newsletter. As a result the following key decisions have been made about future developments.

- Efforts will be made to increase the number of articles on the use of ECMWF products, with contributions from users of such products, particularly within the Member States, being encouraged.

- Once a year, a comparison of the performance of ECMWF models with those from other centres will be published.
- More effort will be put into publishing timely news items.
- The *ECMWF Newsletter* and its availability on the web will be advertised during visits to Member States by ECMWF staff, and the opportunity will be taken to encourage the submission of articles on the use of ECMWF products.

More information about the results of the survey is available from

- <http://www.ecmwf.int/publications/newsletters/survey.pdf>

As indicated in the first of the key decisions, ECMWF is keen for the *ECMWF Newsletter* to include more articles by users of ECMWF products from with Member States and beyond. Advice about preparing articles can be obtained from the Editor by contacting Bob.Riddaway@ecmwf.int. In addition, some guidance for authors is available from:

- <http://www.ecmwf.int/publications/newsletters/guidance.pdf>

Thanks go to everyone that completed the questionnaire. Every effort will be made to use the results of the survey to improve the content and appearance of the *ECMWF Newsletter*.

Operational assimilation of NOAA-19 ATOVS data

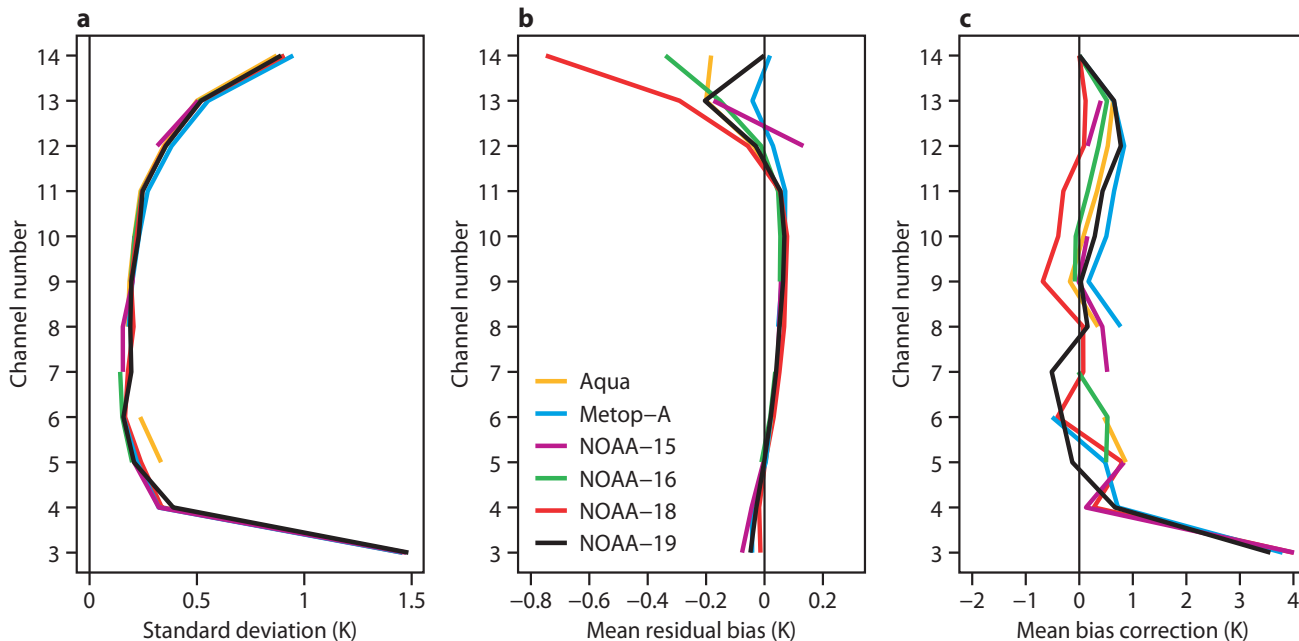
NIELS BORMANN

Sounding data from NOAA-19, the latest and last of the NOAA-series of polar orbiting satellites, has recently been included in ECMWF's operational assimilation system. Following the launch of NOAA-19 on 6 February 2009, data from the ATOVS instruments (i.e. AMSU-A, MHS, HIRS) was evaluated and compared to data from similar instruments as a contribution to the international efforts concerned

with calibration/validation. Overall, the initial monitoring characteristics were broadly in line with expectations and consistent with data from similar instruments already used in the system. Exceptions were more complex scan-bias characteristics for HIRS and AMSU-A. These are not fully corrected by the method used at ECMWF for correcting scan-biases, but the residual bias effects are relatively small.

In assimilation trials, NOAA-19 ATOVS data gave a small positive

forecast impact over the northern hemisphere when added as sixth AMSU-A, fourth AMSU-B/MHS, and third HIRS instruments. While the NOAA-19 orbit is close to that of NOAA-18 or Aqua, NOAA-19 data still provided additional coverage even after the combined thinning with data from all other satellites for the trial period. It is remarkable that a small positive forecast impact is found despite the presence of so many similar instruments in the



NOAA-19 monitoring statistics consistent with data from similar instruments. Global first-guess departure statistics for AMSU-A over sea for the satellites considered in the ECMWF system, in terms of (a) the standard deviation of first guess departures after bias correction, (b) the mean residual observation minus first-guess bias after bias correction, and (c) the mean bias correction. For NOAA-19, statistics are based on passively monitored data after quality control, whereas for the other satellites statistics are shown for assimilated data or passive data that is used for quality control. Statistics are based on the five-day period 21 to 25 April 2009 and they have been taken from the operational assimilation system.

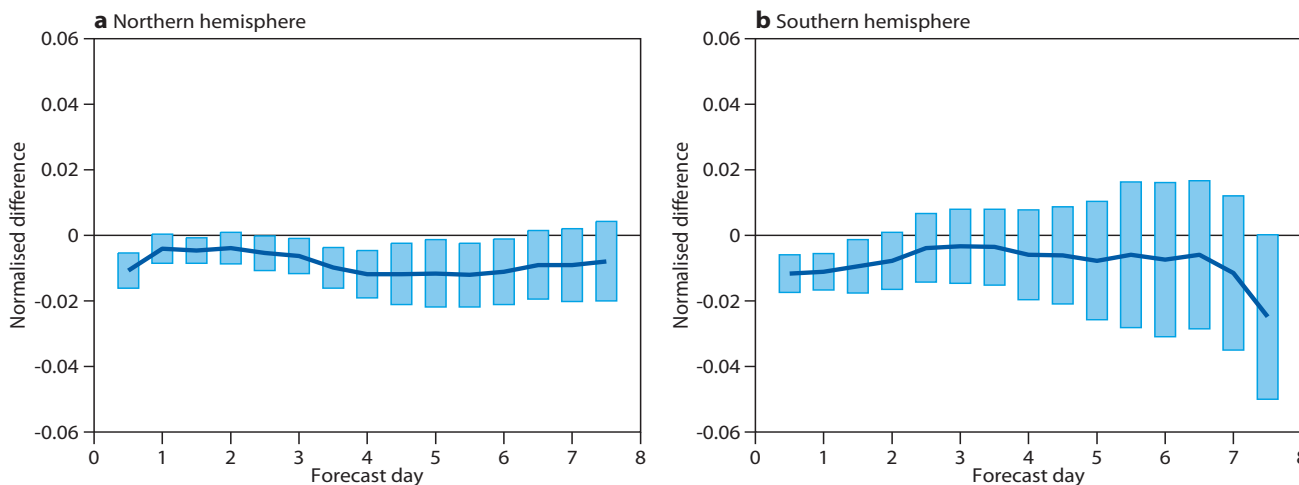
assimilation. NOAA-19 ATOVS data has been assimilated operationally at ECMWF since 2 June 2009.

Soon after its introduction in operations at ECMWF, the MHS instrument on NOAA-19 has, however, already shown signs of degradation in some channels, with an increase in noise over time. The reasons for the degradation are still under investi-

gation at the satellite agencies. The situation was closely monitored at ECMWF, and the instrument was excluded from the assimilation on 4 August 2009 when the instrument noise exceeded the specification for the affected channels. Also, the orbits of NOAA-18 and NOAA-19 have now drifted even closer together, such that little additional coverage is

provided by AMSU-A.

The sounding capabilities provided by the NOAA-series of satellites will be continued and enhanced through future instruments on the NPOESS platforms, the USA's next generation of low earth orbiting environmental satellites, and on its precursor mission NPP (NPOESS Preparatory Project) that is due for launch in 2011.



Impact of NOAA-19 data on forecasts. Normalised differences in the root mean squared forecast error between the NOAA-19 experiment and the control for the 00 UTC forecast of the 500 hPa geopotential for (a) northern hemisphere and (b) southern hemisphere. Negative values indicate a reduction in forecast error and therefore a positive impact of NOAA-19 data. Verification is against the own analysis, and the period is 28 March to 18 May 2009 (52 cases). Error bars indicate 90% significance intervals from a t-test.

Thirty years of world-class weather forecasts

MANFRED KLÖPPEL

ECMWF delivered its first operational medium-range weather forecast to its Member States on 1 August 1979. Substantial progress in medium-range weather forecasting has been made over the past 30 years. Nowadays, a forecast for five days ahead is of the same quality as a forecast for two days ahead in August 1979. During this period there have been impressive improvements in the early warning of severe weather; this is one of the primary objectives of the current ECMWF strategy.

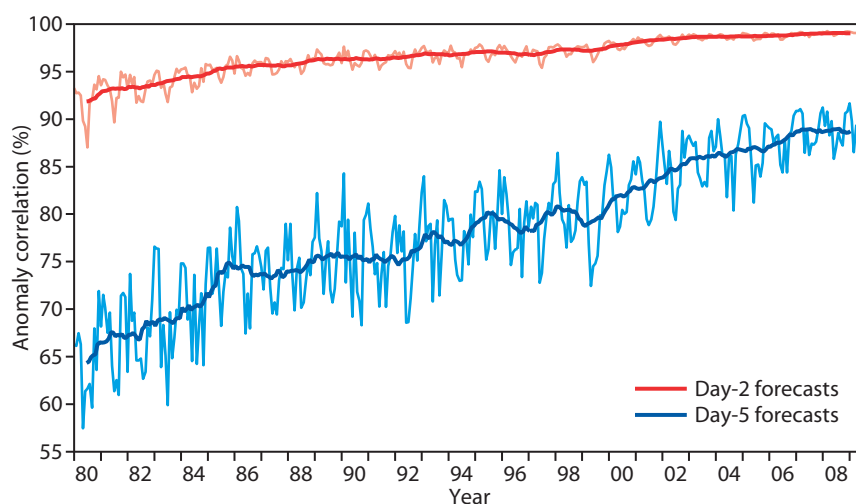
The forecast system introduced in 1979 was shown to be the best in the world and ECMWF has been in a leading position since then. The science behind weather forecast modelling is as important as advances in computer technology for the success of ECMWF. Through systematic model development and increased use of satellite and in situ observations, the ECMWF forecasting system continues to improve. In addition to enhancing the quality of the forecasts over the thirty-year period, there have been significant developments in the range of products provided and in operational efficiency. All these developments have been of benefit to the Centre's Member States and Co-operating States.

ECMWF's first supercomputer, a CRAY-1A, was a single processor computer with a memory of 8 Mbytes. In peak performance terms, the ECMWF's current computer system is almost two million times more powerful than the CRAY-1A. The current High Performance Computing Facility is one of the most powerful in Europe.

The success of ECMWF has been built upon the high-level of expertise of its staff, its leading role in using high performance computing in meteorology, the fruitful relationship between ECMWF and its Member States and Co-operating States, and the long-lasting collaboration with other international organisations and the research community.



ECMWF supercomputers. The CRAY 1-A (top), the first supercomputer at ECMWF, and the current IBM supercomputer (bottom).



Accuracy of the ECMWF forecasts. Increase in the anomaly correlation for day-2 and day-5 forecasts of 500 hPa geopotential from 1980 to date for the northern and southern hemisphere extra-tropics. The monthly figures are shown along with the 12-month moving averages.

The new all-sky assimilation system for passive microwave satellite imager observations

PETER BAUER, ALAN GEER,
PHILIPPE LOPEZ, DEBORAH SALMOND

WITH THE operational implementation of IFS cycle 35r2 (Cy35r2) on 10 March 2009, a new system for the assimilation of passive microwave imager radiances was introduced. The microwave imager radiances are sensitive not just to atmospheric moisture and surface wind speed, but also to clouds and precipitation. Most of the data is contributed by the Special Sensor Microwave Imagers (SSM/I onboard DMSP satellites; available since 1987) and the Advanced Microwave Scanning Radiometer (AMSR-E onboard the Aqua satellite,

available since 2003), and will be complemented by further satellite instruments in the future.

The all-sky system represents the first framework in which satellite radiances are not separated into clear-sky and cloud-affected streams. All radiances are treated with the same observation operator, which produces increments for all the above physical fields and actively drives the moist physics parametrizations. Most other satellite observations are used in cloud-free areas and the cloud screening is performed on the basis of observational information only. This may produce a sub-optimal sampling in situations where observations are clear but the model forecasts clouds; a disadvantage that is overcome with the all-sky system.

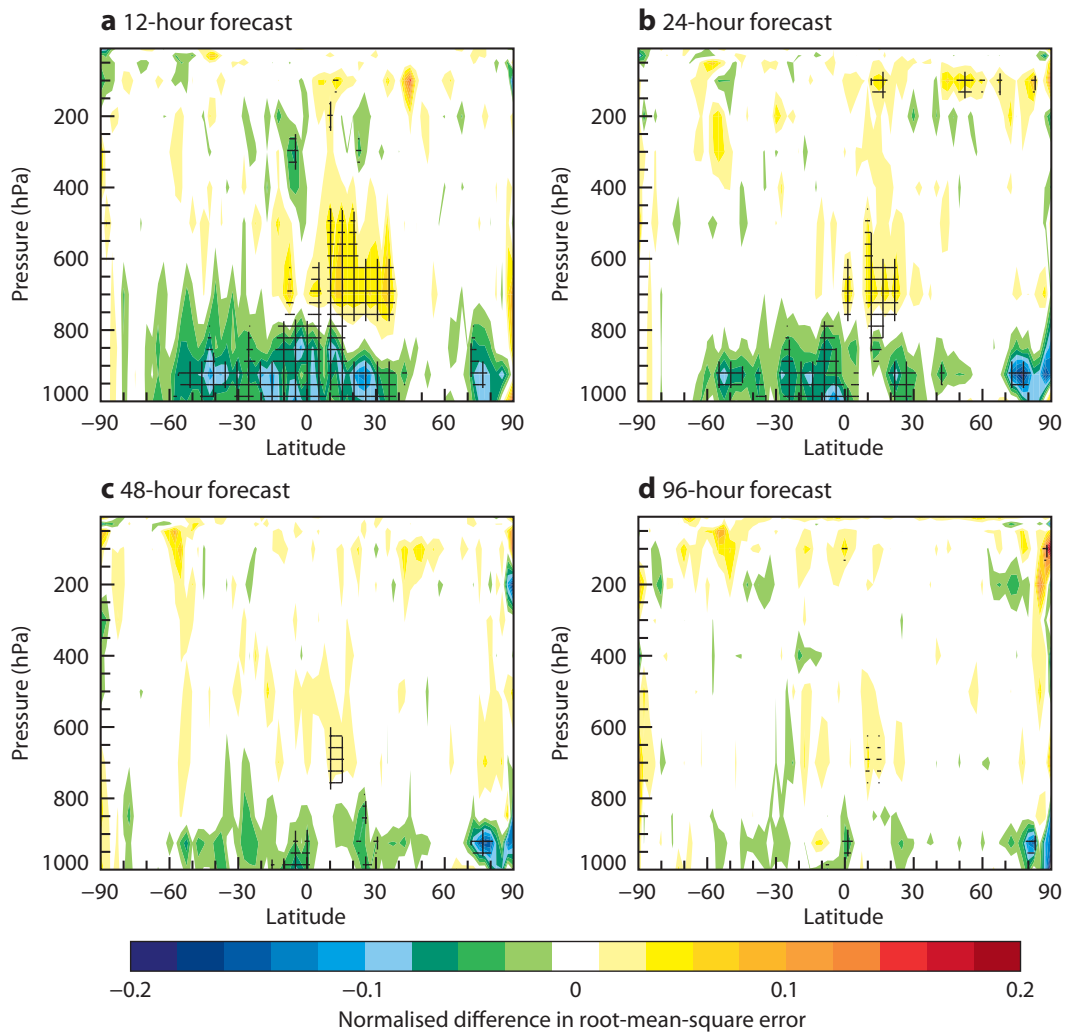


Figure 1 Normalised difference between All-Sky and Control experiments for the root-mean-square forecast error for relative humidity verified against own analyses for (a) 12-hour, (b) 24-hour, (c) 48-hour and (d) 96-hour forecasts. Blue colours indicate where the All-Sky experiment has smaller forecast errors than Control. Cross-hatching indicates differences significant at the 90% level.

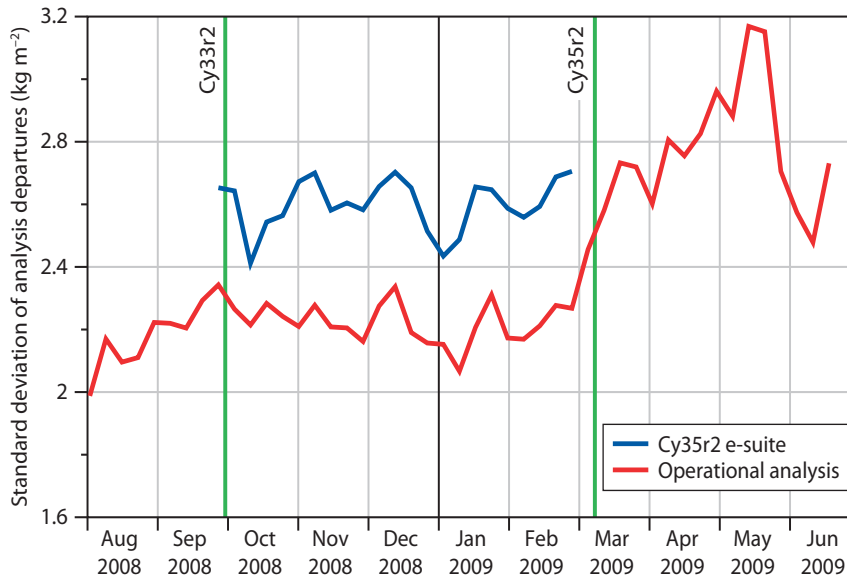


Figure 2 Standard deviation of analysis departures of total column water vapour from the Envisat Microwave Radiometer, calculated over the tropical region.

Substantial effort has been spent on the improvement of the observation operator, channel selection, the definition of observation errors and bias correction. The system also required the activation of the moist physics parametrizations in the first minimization of the 4D-Var assimilation process. As a result of all these changes, more microwave imager observations are used than before.

Figure 1 demonstrates the impact in terms of the normalized forecast error difference for relative humidity between the new system and a control experiment for five weeks in August–September 2008. The control experiment employed separate treatments of microwave imager observations in clear-sky and cloud-affected areas, the latter through the 1D+4D-Var assimilation system (*ECMWF Newsletter No. 110*, 12–19). The scores suggest a large improvement in the lower troposphere across all latitudes that is maintained until day-2 of the forecast. At mid-levels in the tropics a deterioration is found that is most likely related to larger variability due to a weaker constraint of observational humidity by the all-sky system compared to the 1D+4D-Var. Wind and temperature scores are rather neutral and the general fit to both satellite and radiosonde moisture observations in the analysis and short-range forecast is also largely unchanged. This means that the new assimilation of microwave imagers is producing similar forecast benefits to the previous one. These benefits are seen mainly in short-range tropical wind and moisture forecasts.

Figure 2 shows the time series of departure standard deviations between model analyses and independent total

column water vapour observations obtained from the Microwave Radiometer (MWR) onboard Envisat. The Cy35r2 e-suite, in which the all-sky system has undergone pre-operational testing, constrains the moisture analysis less than the operational system, mostly due to a more rigorous quality control. This leads to generally larger analysis departure standard deviations when the all-sky system is used. In the period between April and May 2009, however, both active instruments (DSMP F-13 SSM/I and Aqua AMSR-E) had data outages so that the analysis departures increased by about 15% compared to the independent MWR observations. This trend is only reversed when the SSM/I and AMSR-E data returned in June 2009. This shows that, although the constraint of lower tropospheric moisture is slightly weaker than before, the new system still has quite a substantial positive benefit.

The all-sky system is the first operational 4D-Var assimilation system for clear, cloud and precipitation affected radiances and represents a significant step towards satellite usage in areas which have been largely unexploited until now. It is hoped that further updates will be made with Cy36r2 (due in spring 2010), based on improved bias correction, quality control and observation error definitions. With these it will be possible to increase the weight of the all-sky data in the analysis, thus substantially increasing the constraint of lower tropospheric moisture and cloud. In the future, the system will also be tested with microwave temperature (Advanced Microwave Sounding Unit, AMSU-A) and moisture (Microwave Humidity Sounder, MHS) sounder radiances aiming at a unified all-sky radiance assimilation for all sensors.

Tracking fronts and extra-tropical cyclones

TIM HEWSON

FORECASTERS have long recognized the merits of tracing the evolution of meteorological ‘features’ in the atmosphere – originally in observational data, and increasingly, nowadays, in model output. The motivation for following such features is that, directly or indirectly, they correlate with significant and sometimes severe weather. For example, line convection, a feature seen on radar images, directly relates to heavy precipitation, reduced visibility and squally winds, whilst upper-level PV (potential vorticity) anomalies, features seen in model output, can be an indirect precursor to rapid cyclogenesis and all the adverse weather that entails. The two features most widely recognised in the extra-tropics are, arguably, fronts and cyclones. Analysis of these has historically been a time-consuming manual process; in operations, when there was but one model run to deal with, this was just about tractable, but nowadays, in the era of ensembles, it is plainly not.

Conveniently, mathematical algorithms have been built up, over a number of years, to identify and track such features in an automated fashion. Initially these algorithms were developed at the Met Office and applied to MOGREPS (Met Office Global and Regional Ensemble Prediction System) data. Related output is now part of the suite of operational real-time products provided to Met Office forecasters. More recently this code has been upgraded and applied to forecasts from ECMWF’s Ensemble Prediction System (EPS) to develop products for ECMWF customers. This article describes those products and their origins. We also provide advice on how to use the products in an operational setting, in conjunction with guidance from the higher-resolution ‘deterministic’ model.

The key benefits for the user of this new feature-based approach to ensemble processing are summarised below.

- ◆ Identifying where warm fronts, cold fronts and cyclonic features of different types are in the ensemble, how these propagate with time, how uncertainty (i.e. positional spread) develops in their handling and how this uncertainty varies, on a given day, across the domain of interest.
- ◆ Seeing whether the deterministic and control runs provide ‘mid-range’ solutions, in their handling of fronts and cyclonic features, relative to the rest of the ensemble.
- ◆ Visualising ‘synoptic-chart-style’ animations that show fronts, cyclonic features and mean sea level pressure, for all the model solutions.
- ◆ Distinguishing between cyclonic features of different synoptic types, such as ‘frontal waves’, ‘diminutive frontal waves’ and ‘barotropic lows’, and also distinguishing cold front features from warm front features.
- ◆ Visualising the evolutionary history, in the deterministic and ensemble solutions, of a particular cyclonic feature

in a ‘feature-plume’ format. Components represented include 12-hour movement vectors (i.e. tracks), mean sea level pressure at the feature point, and low-level wind maxima within fixed radii of the feature point.

- ◆ Visualising, as animations, storm track strike-probabilities using three different thresholds for feature intensity. This allows ‘the potential for cyclonic activity’ and indeed ‘potential storminess’ to be diagnosed out to 15 days.

Fronts

Both forecasting practice and theoretical ideas indicate that warm and cold fronts should mark the transition zone between airmasses of different thermal characteristics. Such fronts thus denote regions of large thermal gradient. For consistency with the typical vorticity signature – as denoted at the surface by a wind shift – fronts are actually identified *along the warm air boundaries* of the regions of large gradient.

Two key choices have to be made when identifying fronts – which thermal variable should one use and on which atmospheric level or levels? Following extensive testing, which involved comparison of objective fronts with fronts found on manually-produced synoptic charts, the choice was made to use wet bulb potential temperature (θ_w) on a terrain following co-ordinate that is 1 km above the model topography.

θ_w has valuable conservative properties; in particular it tends to give continuity to frontal progression across elevated topography. A level of 1 km is reasonably representative of the lower troposphere and has a close connection with surface weather, as required, but at the same time is not ‘contaminated’ too much by the underlying surface. One important aim was to avoid seeing semi-permanent fronts around many coastlines – at levels lower than about 1 km this becomes an issue. A pressure level approach was not adopted because surface processes and sub-surface extrapolation would have had a contaminating effect around high topography.

To plot the fronts a number of diagnostics, based on horizontal derivatives of the chosen thermal field, are computed; these are then plotted using standard graphical algorithms. The fronts themselves are merely a contour plot on which some contour segments have been erased. The red and blue colouring, for warm and cold fronts respectively, is dependant on another variable; here the sign of the geostrophic thermal advection is used. This is broadly consistent with forecasting practice in Europe.

Comparison of objective and manually-analysed fronts

Automated and manual analysis charts for one time have been interlaced on Figure 1 to enable synoptic feature posi-

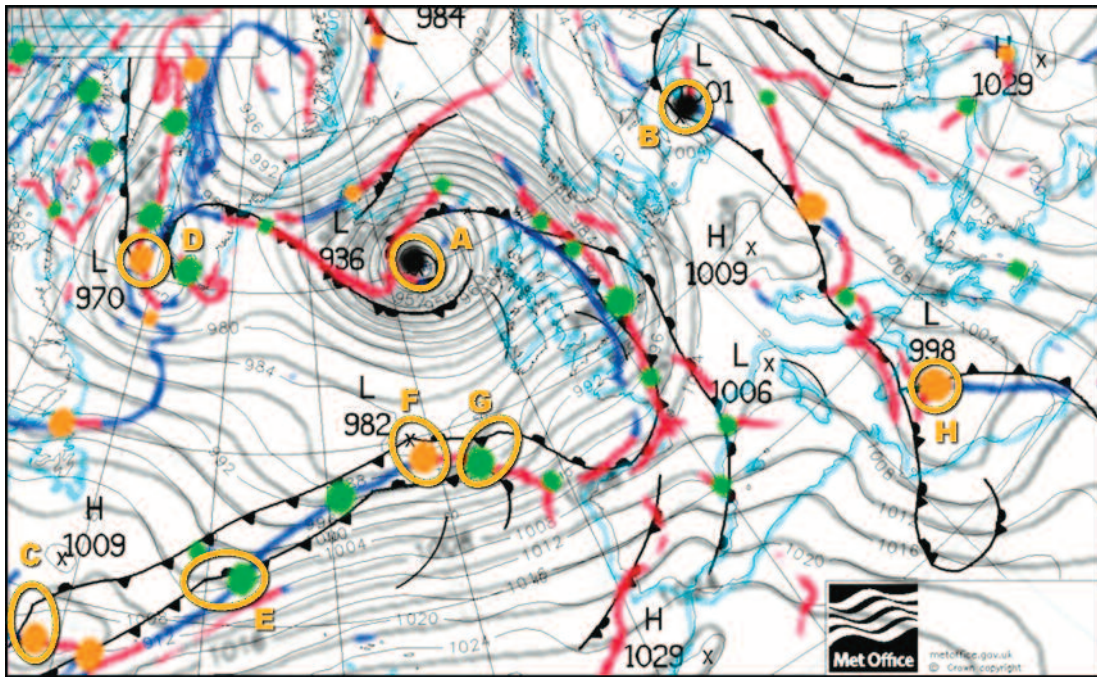


Figure 1 Met Office subjective (black) and ECMWF automated (grey and colour, control run) synoptic analysis charts for 12 UTC on 22 January 2009, blended for comparison. On the objective charts warm fronts are red and cold fronts blue, whilst diminutive waves, frontal waves and barotropic lows are shown, respectively, by green, orange and black spots. Weaker frontal features are shown by smaller spots. Rings highlight cyclonic features that are equivalent on the two chart types.

tions to be compared. Manual fronts are shown conventionally, objective fronts are in colour: good general agreement is immediately apparent. There are some discrepancies however. One concerns smoothness; this is much greater for the manual fronts. An analyst will deliberately smooth out fronts to provide a product that is more aesthetically pleasing, though may at the same time sacrifice some useful local detail. For the automated product there is only slight smoothing of the input fields. A second point is that manual occlusions tend to be denoted by objective warm fronts. Thirdly, note that a few fronts, both manual and objective, do not have counterparts. This will be partly because an analyst can take into account additional factors, such as cloud bands on imagery, or visibility gradients, when identifying fronts. As discussed above, the objective method uses only wet-bulb potential temperature, in the expectation, from experience and frontal theory, that these other delineations will be broadly coincident most of the time.

New animated web product – ‘spaghetti fronts’

Figure 2 shows example frames from an animated web product being developed for users, which we call a ‘spaghetti fronts’ animation. It depicts objective fronts in all members, at different lead times, from one EPS run in summer 2009. The evolution from a coherent pattern, with good inter-member agreement at short leads (Figure 2a) to a random-looking pattern by long leads (Figure 2c) is typical. At long lead times only climatological aspects – such as the absence of fronts in the tropics – tend to stand out. What we are effectively doing here is representing trends in the EPS spread in a synoptically meaningful way (i.e. as they relate to frontal positioning). Questions the user can address with this product include the following.

- ◆ How confident are we in the positioning of different fronts at particular lead times? In Figure 2a confidence in the position of the warm front southwest of Greenland is evidently higher than confidence in the fronts northwest of Norway.
- ◆ How representative of the ensemble are the control and deterministic runs? Control run fronts are always overplotted in green and gold. Figure 2b indicates that a cold front will likely be crossing Northwest Europe around T+180 hours; the control run seems to be mid-range and so should be ‘reasonably representative’ of the ensemble for this particular feature, and by implication for the general weather in this region around this lead time.
- ◆ At what lead does making any sort of deterministic prediction become futile? One could argue that, away from arctic regions, there is some confidence in identifying airmass boundaries at T+180 (Figure 2b), justifying a modicum of determinism in forecasts issued for that time. Conversely, by T+360 (Figure 2c) the confidence in where the airmass boundaries will be is virtually nil.

Cyclones

Feature types

Cyclones in the extra-tropics can take on many forms, but commonly they start out as a small cyclonic disturbance on a pre-existing front. Most forecasters would refer to this as the ‘frontal wave’ stage. On a synoptic chart such features lie at the meeting points of cold and warm fronts, with the extra condition that the implied frontal rotation must be in the correct (cyclonic) sense.

Recent work has identified a new type of frontal cyclonic feature, which has been named a ‘diminutive wave’. This is typically a very minor disturbance on a front, which, in the

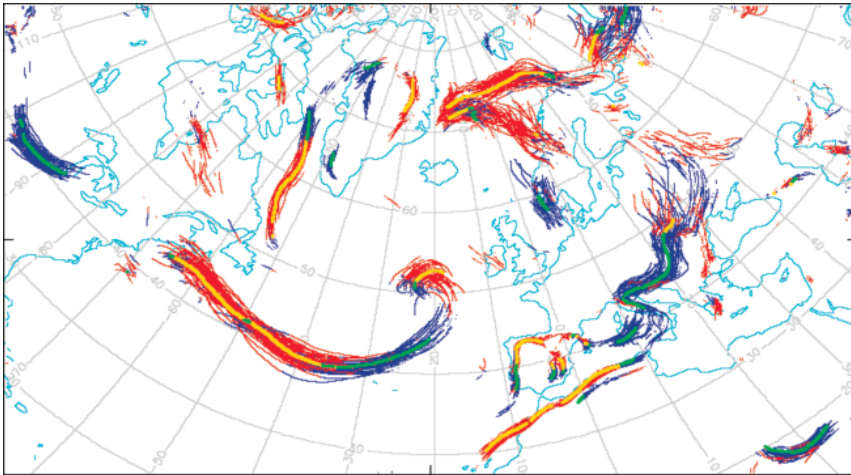
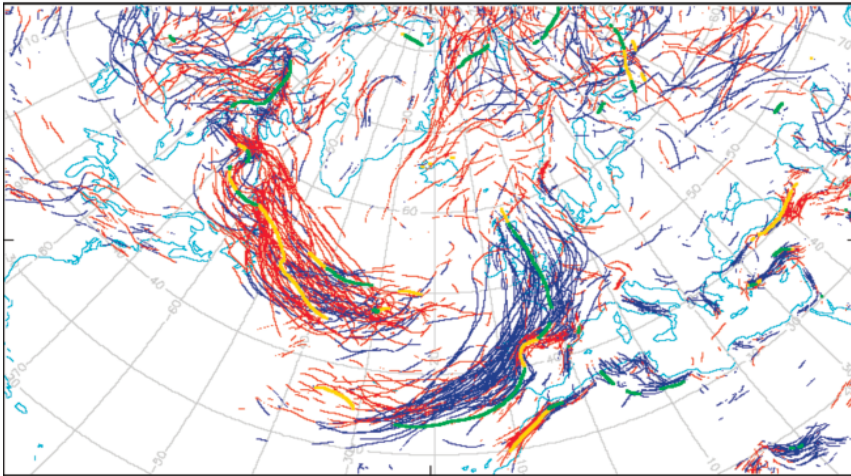
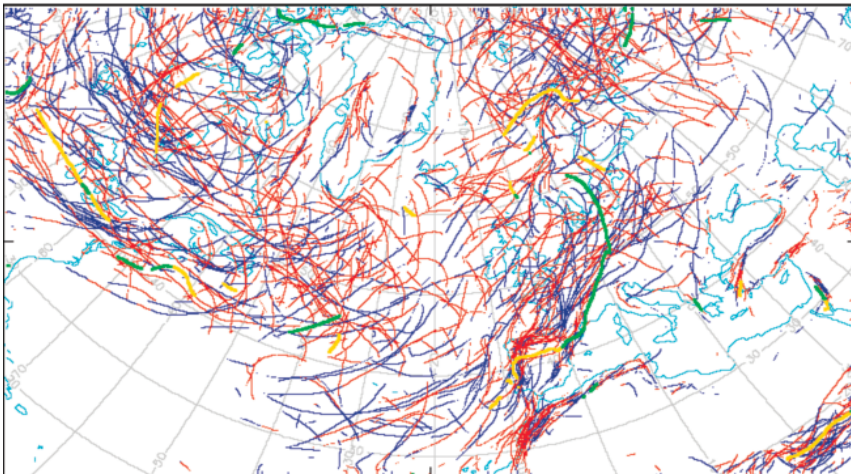
a T+60**b** T+180**c** T+360

Figure 2 Objective front spaghetti plots, from one set of ensemble runs, data time 00 UTC on 23 July 2009. Lead times are (a) 60 hours, (b) 180 hours and (c) 360 hours. Control run fronts are shown in gold (warm) and green (cold). Fronts from the deterministic run are not shown here, but will be incorporated onto standard products in the near future (up to T+240).

cyclone life-cycle, tends to precede the frontal wave stage. It can be recognised, synoptically, by a slight opening out of the isobars along a front. Dynamically, this opening out signifies the development of a local positive-negative couplet in the vorticity of the cross-front geostrophic wind; it is the maximum in this quantity – the positive part – that pinpoints the diminutive wave (see also Box A). If a diminutive frontal wave develops further, then a frontal segment on one side

will change to a different (warm or cold) type, and at this point it will have transitioned into a frontal wave. Then if the frontal wave further intensifies it will eventually lose its thermal (frontal) signature as it evolves into a non-frontal low pressure centre. This we refer to as a *'barotropic low'*.

Figure 3 depicts a conceptual model of the life cycle of a cyclonic feature that initially forms as a diminutive wave on a warm front, then passes through the stages mentioned

The dynamical significance of diminutive frontal waves

At first sight diminutive frontal waves seem to be such small features that one might imagine that they are dynamically inert. Conversely the fact that many can be tracked in a coherent fashion, and that some develop substantially, suggests otherwise. One ensemble example of a modest development that could be tracked in time, and that led to severe weather, is shown in the figure.

In terms of dynamical forcing, the locally splayed out isobaric pattern that one tends to see around diminutive waves (e.g. stage 1 in Figure 3 and the inset in the top-left panel of the figure below) can be interpreted in two ways.

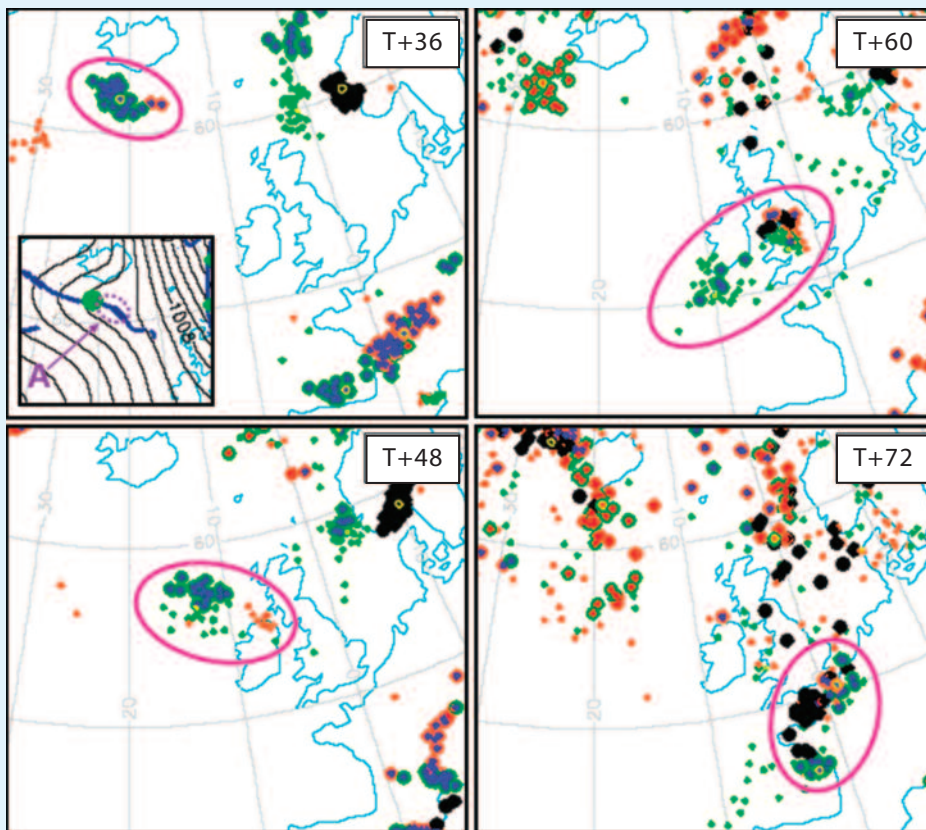
(a) This pattern is akin to a deformation pattern that, when acting on isotherms that are typically front-parallel, will be frontogenetic. Such patterns are associated with forced ascent. For a diminutive wave, where the along-front extent of the deformation pattern is limited, there will preferentially be forced ascent just in the region of the deformation (e.g. area 'A' on the figure). Other things being equal this would lead, for example, to higher precipitation rates near to the associated frontal segment.

(b) For a warm front diminutive wave there will be a local

maximum in warm advection on the high pressure side of the wave. For a cold front diminutive wave there will be a local minimum in cold advection on the low pressure side. In a standard quasi-geostrophic omega equation treatment of dynamical forcing, the Laplacian of the thermal advection field represents one part of the forcing for ascent. In these cases the maximum in warm advection and the minimum in cold advection both contribute positively to this Laplacian term, and thereby also contribute positively to locally forced ascent. So again, other things being equal, one would expect higher rain rates near to the respective front segments.

It is tempting to also try to apply the above arguments to the case of cold front waves (see Box B), though the complicating effect of variations in along-front thermal gradient, particularly for more developed features, makes this less appropriate.

The lesson is that forecasters should not readily dismiss diminutive waves as insignificant, inert features. Some, certainly, will turn out to be, but others can be very important even if they do not develop markedly.



Synoptic cyclonic features. A cold front diminutive wave in the ensemble (green spots with a blue centre) moves southeast towards the UK, and in some members develops further into a cold front wave (orange spot with blue centre) and/or a barotropic low (black spot). This feature gave rise to a very rare early snowfall over Southeast England on the evening of 28 October 2008 (between about T+66 and T+72). Top left inset shows the automated synoptic chart from one member; 'A' denotes a region of inferred forced ascent. The legend in Figure 5 gives the meaning of all symbols.

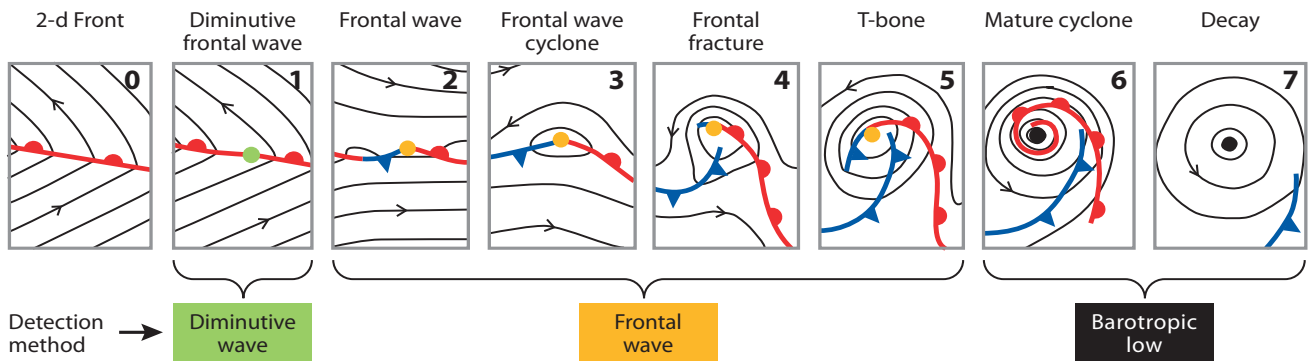


Figure 3 Conceptual model of the life-cycle of a cyclonic feature that develops on a warm front. Stages 3 to 6 come from the Shapiro-Keyser conceptual model; others have been added. Spot colours signify the detection methods used for the different stages.

above, before eventually decaying. A similar model could portray a feature that initially develops on a cold front.

The above discussion suggests that a 'typical' cyclone life-cycle in the extra-tropics can consist of a number of stages. At the same time, however, it is important to recognise that most cyclonic features will not evolve in the way shown by Figure 3 – for example, some will decay at a very early stage. Others meanwhile could start out as a barotropic low – given, say, large upper-level forcing in the absence of surface fronts. The identification and tracking strategies detailed below cater for all such eventualities.

Feature identification

In order to objectively recognise and track, in model output, cyclonic features, and at the same time make a strong connection with synoptic forecasting practice, separate sets of mathematical algorithms have been developed to identify each of the three feature types (annotated at the foot of Figure 3). On the automated synoptic charts these cyclonic features are denoted by spots (this approach was used for Figure 1 and the same convention is used on charts referred to later in the case study). Post-processing forces there to be a minimum separation of ~300 km between features and concurrently enforces a decision hierarchy: frontal waves take precedence over barotropic lows and diminutive waves, and barotropic lows also take precedence over diminutive waves.

Comparison of objective and manually-analysed features

On Figure 1 agreement between objective and subjective cyclonic features (see rings) is generally good. On the automated chart barotropic lows (A, B) tend to be in exactly the right place, and frontal waves are usually close to their counterpart (C, D, E, F, G, H). However there are some differences between the charts. The most striking is that there are rather a lot of unmatched objective features, most of which are diminutive waves. One reason for this is that as yet the synoptician has no symbol available to denote such a feature. Occasionally, if they think a cyclonic disturbance is developing, a frontal wave can be 'concocted' on a front in between the isobars, where arguably a diminutive wave should have been shown – waves E and G are perhaps cases in point.

Feature C on Figure 1 denotes the beginnings of wind-storm 'Klaus', which hit France and Spain 1–2 days later.

Analysis in the vicinity of such systems can be difficult, so it is reassuring that both objective and subjective means picked this up.

Feature tracking

After identifying where the cyclonic features are at each time, we next want to connect up associated features on successive charts to construct tracks. This is a non-trivial process and requires accurate estimates of 'association probability' to derive meaningful tracks that the synoptician will believe. The first stage of the process involves progressing and retrogressing features on consecutive charts, to try to meet up at 'half time'. The translation vectors applied are based on a 'steering wind' (equal to a fraction of an upper-level wind vector) and on previous movement if available. The association probability is then calculated for all possible feature pairings. This depends on three parameters:

- ◆ Feature separation at 'half-time'.
 - ◆ Type transition.
 - ◆ Thickness change (1000–500 hPa) at the feature point.
- In short, each of the following increases the association probability: close matches in space, type transitions that historically (in a manually-analysed training period) have been relatively common, and small thickness changes. Ultimately, through an iterative process, those pairings that have the highest association probabilities are 'matched'; thence they form part of a track, though at the same time care is taken to not track two features into one, and vice versa. In addition if association probabilities for a given feature are all too low then potential matches are discarded, which ensures that tracks have both start and end points.

Tropical cyclones

Though initially developed for the extra-tropics, our algorithms also succeed in locating and tracking tropical cyclones, which are classified as barotropic lows. Tracking works in the tropics, and also through 'extra-tropical transition' should that occur. During such a transition a cyclone typically evolves into the frontal wave feature type.

User products

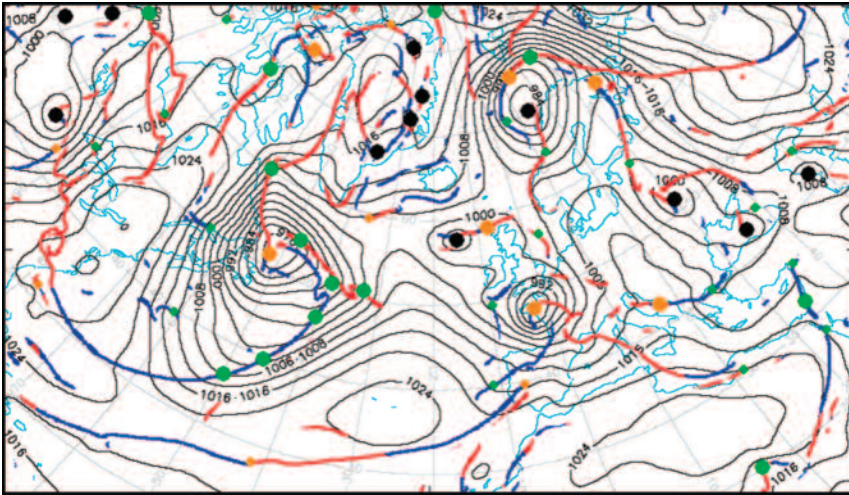
Once we know the feature points and the feature tracks, there are many ways that this information can be usefully conveyed to the forecaster. The simplest way is to just display

automated synoptic charts, in either postage stamp or animation format, and products like this are indeed a key part of the output (an example is given in Figure 4 that is used later in the case study). A recent innovation, to complement the animated front ‘spaghetti plots’, is an animation that shows just the feature points from all the EPS members. We call these

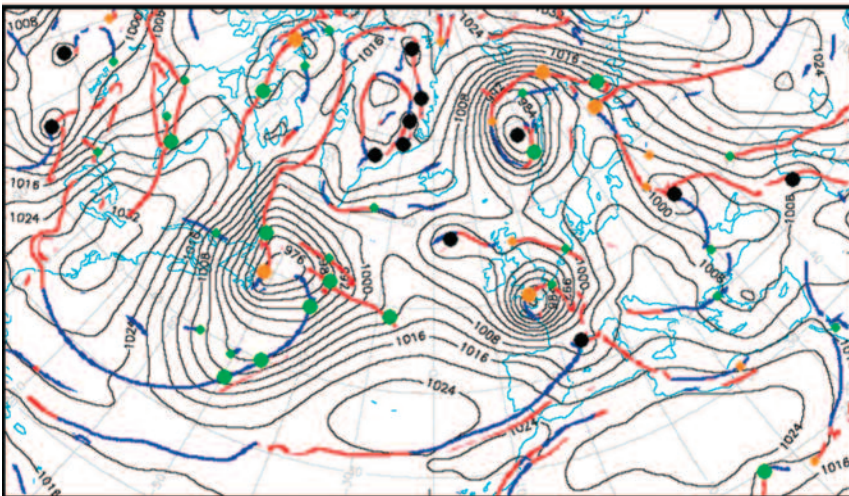
‘dalmatian plots’ (see the figure in Box A, and also Figure 5 used in the case study).

Two different strategies are adopted for presenting track information to the user. Which one is most appropriate depends on the lead time. At time zero, it is usually very easy to cross-reference features in the members; in turn this

a Deterministic forecast



b Control forecast



c Ensemble member 21

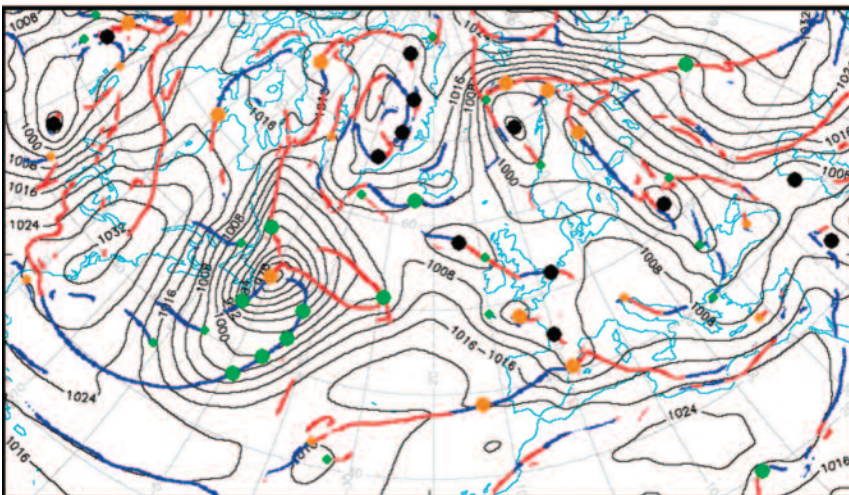


Figure 4 ‘Automated synoptic charts’ at T+120 (00 UTC on the 10th) from data time 00 UTC on 5 February 2009 for (a) deterministic run, (b) control run and (c) ensemble member 21. Colour convention is as specified in Figure 3 and the mean sea level pressure is in black. Weaker frontal features are denoted by smaller spots.

enables 'feature-specific plume diagrams' to be put together, showing how a particular synoptic feature, and various characteristics that it possesses, evolve within the ensemble (see Figure 7 used in the case study). For upcoming significant (cyclone-related) weather events this approach aims to usefully portray the expected life-history of the responsible feature.

At longer leads, as the ensemble spreads, cross-referencing becomes increasingly difficult, and so instead we create storm-track strike-probability plots. In this approach all the tracks, of all the features, are divided up into three sets. The first set – 'all features' – contains every track. The second set – 'stronger features' – consists only of those features for which the wind within their circulation exceeds a certain threshold. The third and final set – 'storms' – is like the second set, but with a higher threshold. The final product comprises a separate animation, for each set. Using colour shading each of these shows the probability that a cyclonic feature, around which the wind exceeds a certain threshold, will pass within a distance of 300 km within a time window of ± 12 hours of frame time (see Figure 6 used in the case study).

How to use the new products – a case study

Here we present a case of 'potential severe weather'. Consider a forecaster who has to prepare forecasts for a Monday night, 9–10 February 2009, for France and the UK.

Thursday 5 February

First imagine that it is Thursday the 5th, and that the 00 UTC products have just become available. It is assumed below that the forecaster would naturally also incorporate information from other ECMWF products and other models as necessary.

What do the deterministic and control runs show?

First there is merit in looking at the automated synoptic chart sequences from the deterministic and control runs. Figures 4a and 4b show snapshots from these for the night in question. There is evidently potential for a deep cyclone to develop, bringing severe winds on its southern flank, as well as heavy rain generally, and also snow on the northern flank if the airmass there is cold enough. Both animations show the cyclone developing rapidly from a cold front wave, though the control run provides the most intense solution.

How typical are the control and deterministic runs?

To address this question we can refer to the 'dalmatian charts', showing where cyclonic features are at different leads. Figure 5 shows the T+120 chart. Evidently a high proportion of members have cyclonic features over northern France and the English Channel. Most are standard frontal waves; some are barotropic lows. Mostly the frontal waves are classified as 'cold front' features, suggestive of strong winds on the western and southwestern flank, as is commonly seen with destructive European cyclones. Box B explains this connection.

The deterministic run feature (shown as a bright green ring and arrowed on Figure 5) is clearly at the southern edge of a feature cluster, whilst the control run (in yellow and also arrowed) is at the northern edge. Thus in this instance,

Cold front wave or warm front wave?

B

For both frontal waves and diminutive waves the identification system is able to classify whether they are cold front features or warm front features. So how is this done?

For the diminutive waves it is trivial, as only one objective front type is involved. For the frontal waves however classification is more involved – it depends on the front-normal geostrophic flow 200 km out from the feature. If this flow, on the cold front side, is greater than it is on the warm front side then the feature is classed as 'lying on a cold front' and vice versa. This broadly accords with synoptic practice. The asymmetry implied in this distinction can be helpful to the forecaster – stronger flow on the upstream side, as with cold front waves, can relate to interaction with a trough and/or PV anomaly at upper levels, and incursion of a dry slot on water vapour imagery. Damaging surface winds can occasionally result.

The dynamical explanation for this behaviour is that upper troughs generally exhibit positive vorticity advection ahead and negative vorticity advection behind. In turn, alluding to the omega equation, we see that this relates to a forcing couplet with forced ascent ahead and forced descent behind. The close juxtaposition of these different forcing regions can help enhance the pressure gradient at the surface, and so as an upper trough catches up with a low, it is commonplace for the aforementioned cold front wave characteristics to develop.

Meanwhile warm front waves (which a dynamical meteorologist might refer to as a 'diabatic Rossby wave') tend to be more confined to the lower troposphere, are more driven by warm advection forcing, and though they may produce copious amounts of precipitation, tend not to develop rapidly. The strong warm advection forcing relates to the stronger flow on the warm front side.

Thus the strong connections between surface synoptic feature type and upper-level interaction should make the provision of classification information to the user, via the 'dalmatian charts', all the more useful to the forecaster.

presuming that we gave equal weight to deterministic and control, and some weight also to each of the other members, the feature would be forecast to lie slightly to the east of a point midway between the two arrowed features. In this way dalmatian charts can be particularly helpful for constructing a 'consensus forecast chart' for a particular time.

What is the likely track of the cyclone, and what is the probability that destructive winds will develop?

Whilst many members seem to be showing features that closely resemble the control and deterministic runs, we do not know from the dalmatian chart exactly how many there are, nor their intensity, nor their direction of movement (though animating can help). So the next product to examine would be a storm track strike probability plot for the

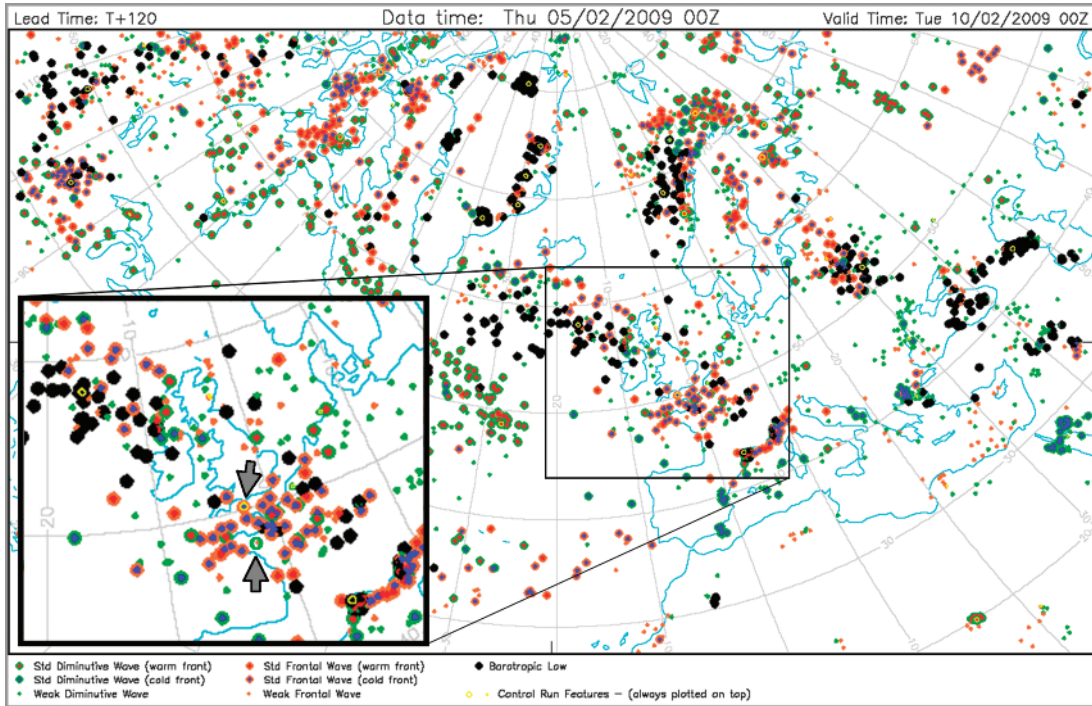


Figure 5 ‘Dalmatian chart’ showing positions of all synoptic features, in all EPS members, at T+120 (00 UTC on the 10th) from data time 00 UTC on 5 February 2009. Symbol style and colour denote type of synoptic feature as in the key below. A portion of the chart has been enlarged, with the position of the main feature in the deterministic run added - see green ring. Other features from the deterministic run are not shown here, but will be incorporated onto standard products in the near future (up to T+240).

highest threshold level (‘storms’) – see Figure 6. This suggests 80% probability of a windstorm-inducing cyclone tracking eastwards in the vicinity of northern Brittany, which could be sufficient justification for warning issue for the parameters discussed above. In general if the control and/or deterministic runs are outliers, then this probability would be less valid, though from Figures 4 and 5 that was clearly not the case here.

What are the other scenarios?

For completeness one should also examine other possibilities. This can be done, at a glance, by referring to synoptic postage stamp charts for T+120 (not shown). This process showed a number of members in which cyclonic development was much more muted. The user can click on these postage stamps to see a frame in more detail – Figure 4c shows one of the weaker members. Note the lack of development, and the stark contrast, at least in terms of implied winds, to Figures 4a and 4b. Issued forecasts could refer to this possibility.

Sunday 8 February

Next we will we move forward in time and imagine that it is Sunday evening with products from 12 UTC on that day now available.

Is there a change in the evolution?

We are now sufficiently close to the time of a potential storm that the responsible feature is apparent in both observation and model data. This means that we can use the ‘feature specific plume’ facility. This is accessed on the web site by click-

ing the feature spot on the control run T+0 frame (top-left inset on Figure 7, arrowed). This brings up another web page, shown in the body of Figure 7.

The top-left panel of Figure 7 (which can be animated) shows the tracks of the feature in the ensemble at 12-hour intervals, as well as numbers of members in which the feature was tracked for the first 96 hours. There now looks to be a strong signal for the feature to track further north than previously expected, across the far south of England. Note also that the control run track, plotted on top in pink/green, is now mid-range, suggesting that its evolution (or that of the deterministic run, which was almost identical) could usefully provide deterministic guidance should that be required.

What do the feature characteristics indicate?

Feature characteristics are shown by the smaller panels on Figure 7. Again there is quite good consistency in central pressure (top-right, spread is $\sim \pm 5$ hPa), and maximum 1-km winds in the circulation (within both 300 km and 600 km radii; lower-left and lower-centre panels respectively). Note also that within a 600 km radius the maximum winds exceed, slightly, those within a 300 km radius. This implies (a) a large system that is having an impact well to the south, and (b) near to the track winds may not be as strong. The fact that the low-level vorticity (centre-right panel) reaches a maximum before the pressure reaches a minimum may also signify an expanding slacker core to the system. This information can all be helpful for warning provision.

The maximum 1-km wind diagnostics can provide an *approximate* guide to gust strength at the surface, though note that other factors, such as stability, can play a substantial

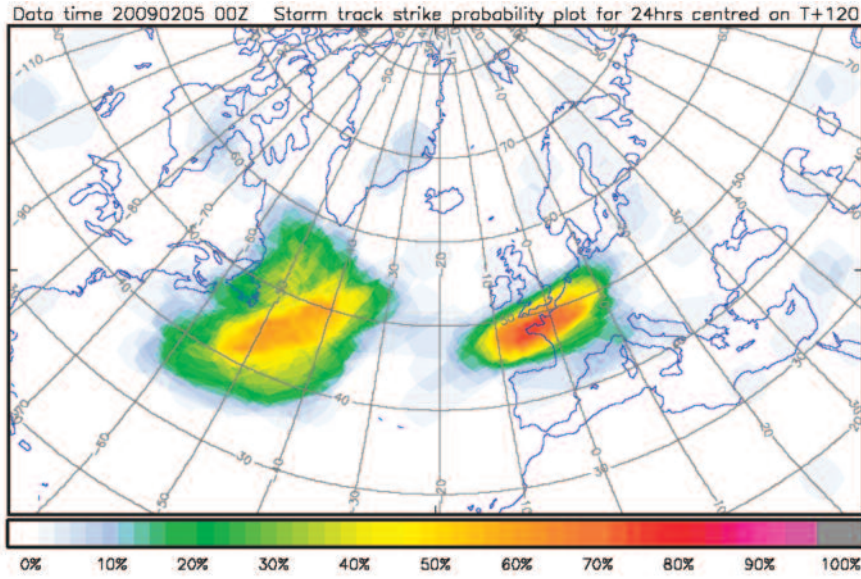


Figure 6 ‘Storm track strike probability plot’ for ±12-hour window centred on T+120 (12 UTC on the 9th to 12 UTC on the 10th) from data time 00 UTC on 5 February 2009. Colours show the probability that a cyclonic feature meeting certain wind threshold criteria will pass within 300 km. The threshold used is that the 1-km wind, within a 300 km radius, must exceed 60 knots during the time window; this is called the ‘storm’ threshold.

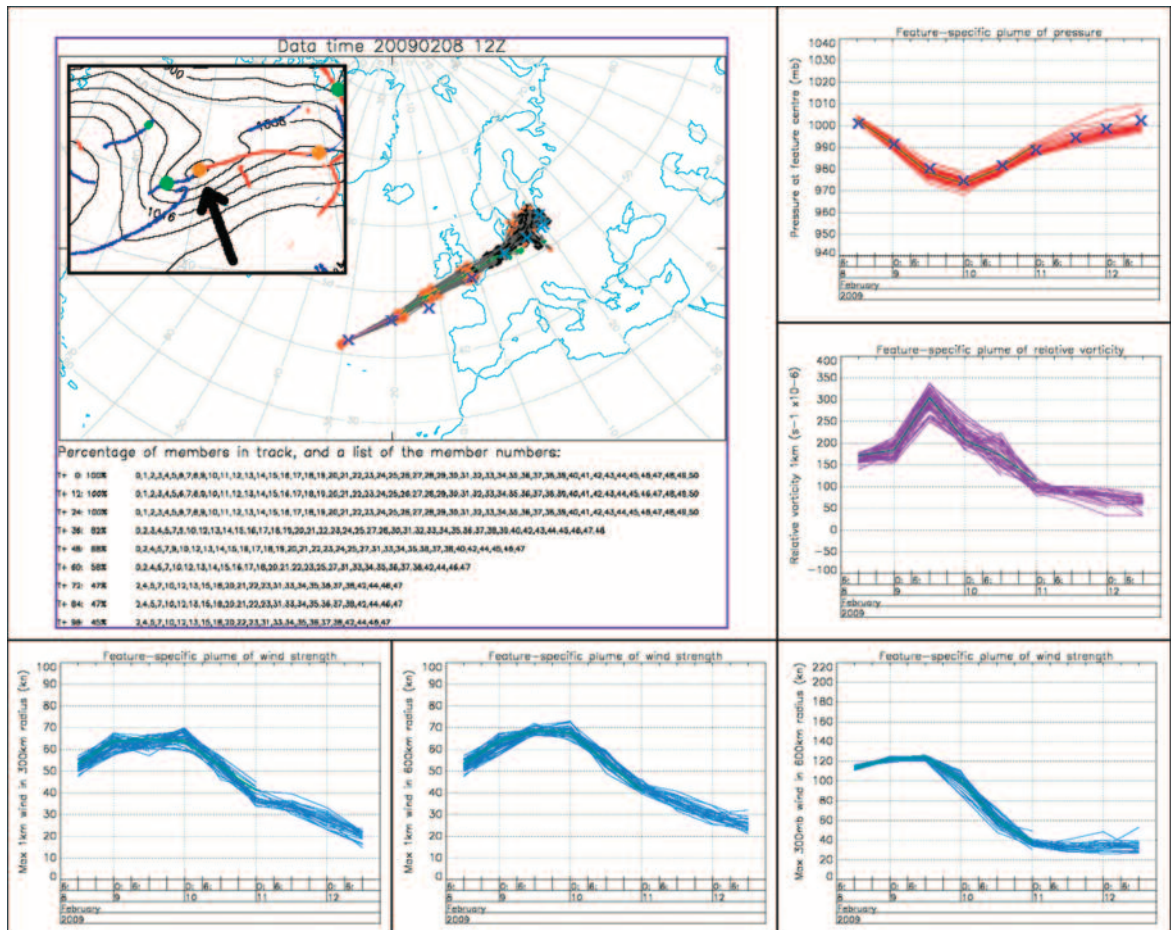


Figure 7 Top-left inset: Segment of the control run automated synoptic chart analysis (T+0 frame) at 12 UTC on 8 February 2009; colour convention is as specified on Figure 3, and mean sea level pressure is in black. The interactive web site allows the user to click on cyclonic features to see their behaviour in the ensemble. Remaining panels show feature plume diagrams for the arrowed (‘clicked’) feature, with verifying data added with blue crosses. Top-left panel: the feature track in the ensemble (this can be animated if the user clicks on the panel) with feature spots at 12-hour intervals. Top-right: feature point mean sea level pressure. Centre-right: relative vorticity at 1 km above the model topography. Lower-left: maximum wind at 1 km within a 300 km radius of the feature point. Lower-centre: same as lower-left but for a 600 km radius. Lower-right: maximum wind at 300 hPa in a 600 km radius.

modulating role. Such diagnostics were mainly designed to provide a general metric of cyclone intensity; in this regard it is advantageous that stability over land and the diurnal variations thereof are not having any modulating effect. Users requiring point forecasts of gust strength, in which stability and wind shear *are* accounted for, can utilise the standard ECMWF ‘maximum 10 m gust’ diagnostic.

Finally, on Figure 7, upper-level jet strength is included in the lower-right panel as an alarm bell for when the forecast surface developments have a higher potential to go awry. Stronger jets are dynamically more active, and there are well-documented cases of ‘forecast busts’ for cyclones associated with these. In extreme cases upper jet strength reaches ~200 knots, so with a 120-knot forecast the error potential here is less than it could be.

What is the probability of a major windstorm?

Finally using Figure 7 the forecaster should note the percentage of members in which the feature has been tracked (top-left panel), but at the same time be mindful that in some cases of cyclogenesis it is not always clear *which* of two successive waves might be developing. All members might be ‘developmental’, though there may be a split decision on which wave will develop. In the inset to Figure 7, for example, the diminutive wave southwest of the arrowed frontal wave could in some members develop instead. The closer one is to feature genesis the more of a problem this can be. So it would be incorrect to infer immediately from Figure 7 that there is only a 68% chance of a major feature existing by T+48.

To support their analysis the forecaster should refer also to strike probability plots from the same data time, which are not feature specific, and which in this case actually show a 100% probability of a major windstorm (Figure 8), with high confidence in its track (much higher, incidentally, than is confidence in the track of storm(s) well to the west).

What actually happened?

Verifying data is plotted on parts of Figure 7 as crosses, showing good agreement, except for feature position at T+24 that lay outside the ensemble range, though not by much. The verifying Met Office analysis for 00 UTC on the 10th is shown in Figure 9. The storm, named ‘Quinten’, is a large feature with a relatively slack core, and shows a nice resemblance to the ‘T-Bone’ stage of the conceptual model in Figure 3. Inland gusts of over 30 ms⁻¹ (60 knots) were widespread between 46° and 48°N over France (tallying quite well with the 1-km wind maxima on Figure 7), whilst there was disruption due to heavy snow and flooding north of the track, over England.

In summary, as this severe event approached, the new products told us that there was an increasing risk of a major storm system in our area, they highlighted the track the system was likely to take, and they also indicated increasing confidence in that track.

Verification

By using, as truth, the cyclonic feature tracks identified in a sequence of analysis frames from either the EPS control run or the high-resolution deterministic run it is possible to verify many of the products illustrated here in an automated fashion. For features tracked from T+0, which have feature plumes, many characteristics can be verified, such as displacement errors, system velocity errors, deepening/filling errors and intensity errors (as denoted by wind strength in the circulation). As well as providing a picture of year-on-year performance changes, such statistics can also guide forecasters regarding how much confidence to attach (on average) to a forecast of a given type of feature, in a given area, at a given lead time. In turn, by comparing the spread in handling of a feature in the current forecast with such statistics one can gain insight into the predictability, in relative terms, of the current situation.

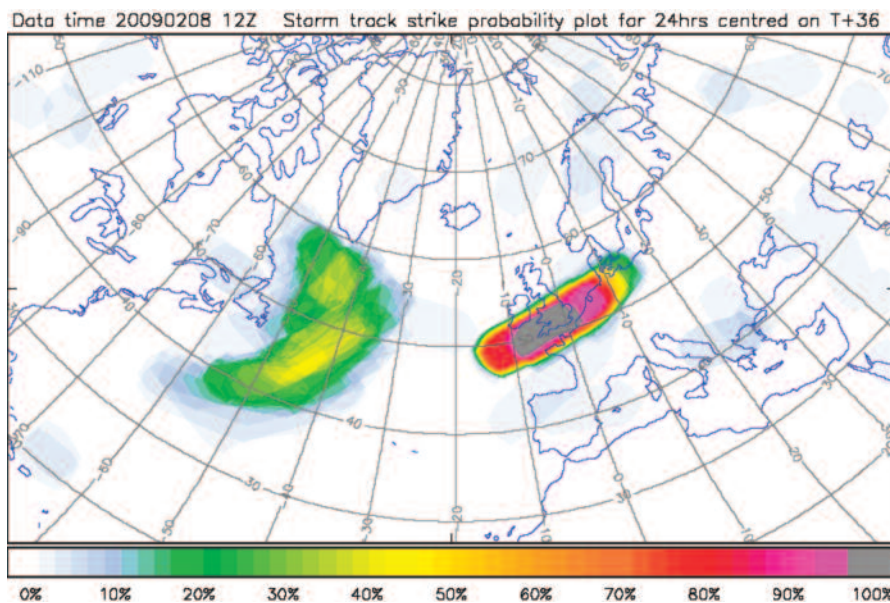


Figure 8 ‘Storm track strike probability plot’ for ±12-hour window centred on T+36 (12 UTC on the 9th to 12 UTC on the 10th) from data time 12 UTC on 8 February 2009. The meaning of the colours is as specified on Figure 6.

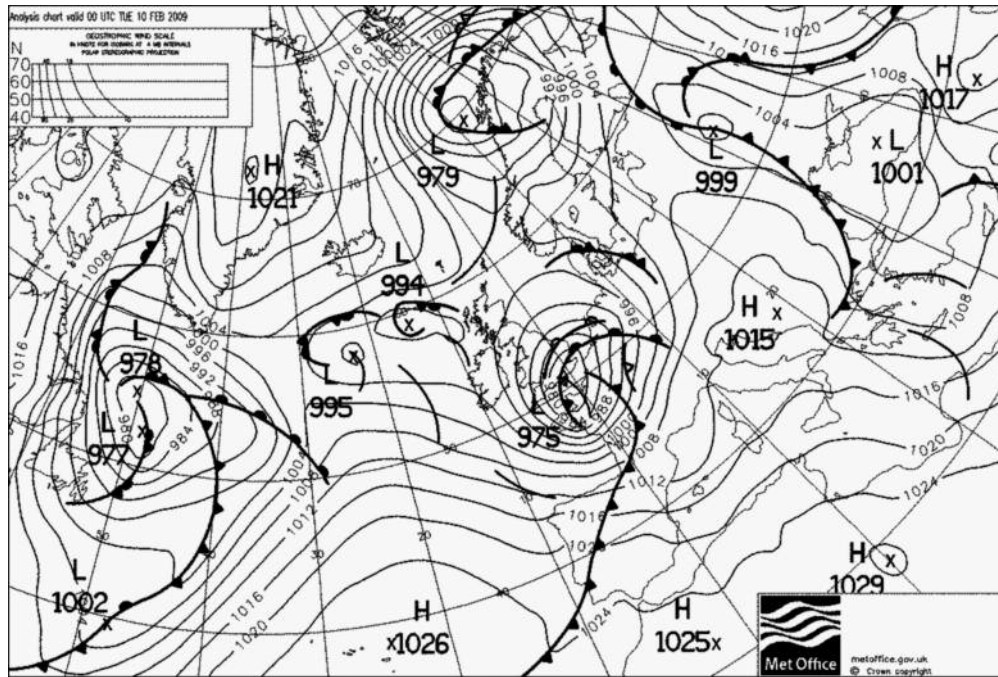


Figure 9 Met Office analysis chart for 00 UTC on 10 February 2009 showing storm 'Quinten' (975 hPa).

More generally, the strike-probability charts lend themselves to verification using a Brier Score approach. At the Met Office, for example, verification of these strike probabilities for the MOGREPS system, over a two-year period, suggested that there was a small degree of skill in predicting the more extreme storms beyond day 10. For those involved in warning provision for windstorms this provides a clear message – that for certain customers who are sensitive to small changes in probability there would be justification for issuing probabilistic severe event warnings at very long leads.

To re-iterate, such verification activities intrinsically focus on aspects of the forecast that are directly connected to adverse surface weather, and so have clear advantages, from a user perspective, over some of the more traditional measures (such as root mean square error in the 500 hPa height). The 'null cases', anticyclones in this case, are implicitly left out. Moreover, by focussing on features which are correlated with adverse weather, we are effectively using a proxy for severe weather verification that, conveniently, does not have associated with it the problems of observation representivity, observation quality control and variable reporting practices that arise when one directly verifies the weather parameters themselves.

New opportunities and further developments

Through a new feature-based approach to post-processing ECMWF is now developing a suite of new products that provide fresh insights into ensemble handling.

A key attraction, for the user, of this new strategy is that the products use the synoptic 'language of forecasters', by focussing on fronts, cyclonic features and cyclonic feature tracks. The inherent automation should vastly reduce the amount of time the user needs to spend analysing the

ensemble and deterministic output. Because 'features' have historically been used, in part, to highlight the potential for severe weather to occur, these new products inherently focus, by proxy, on this potential. This is despite the fact that the finite resolution of the model precludes a direct representation of many of the adverse weather phenomena themselves (e.g. line convection on a cold front). Verification of severe weather 'by proxy' is another significant opportunity that arises from this work.

From a product perspective further developments are planned. Firstly we will incorporate deterministic model output where appropriate. Then on the plume diagram web page other 'attributes' such as precipitation maxima and 10-metre gust maxima are likely to be added, with direct access to 'representative member' animations also provided. The dalmatian plot range should be expanded to signify other aspects, such as feature point mean sea level pressure, using a colour scale.

In concluding we acknowledge the significant contribution of Helen Tittle at the Met Office, who first developed many of the track-related products described here.

Operational implementation of the products discussed in this article is expected in the first half of 2010.

FURTHER READING

- Hewson, T.D., 1997: Objective identification of frontal wave cyclones. *Meteorol. Appl.*, **4**, 311–315.
 Hewson, T.D., 1998: Objective fronts. *Meteorol. Appl.*, **5**, 37–65.
 Hewson, T.D., 2009: Diminutive frontal waves – A link between fronts and cyclones. *J. Atmos. Sci.*, **66**, 116–132.
 Hewson, T.D. & H.A. Tittle, 2009: Objective identification, typing and tracking of the complete life-cycles of cyclonic features at high spatial resolution. Submitted to *Meteorol. Appl.*, May 2009.

Progress in the implementation of Hydrological Ensemble Prediction Systems (HEPS) in Europe for operational flood forecasting

HANNAH CLOKE, JUTTA THIELEN, FLORIAN PAPPENBERGER, SÉBASTIEN NOBERT, GÁBOR BÁLINT, CRISTINA EDLUND, ARI KOISTINEN, CÉLINE DE SAINT-AUBIN, ERIK SPROKKEREFF, CHRISTIAN VIEL, PETER SALAMON, ROBERTO BUIZZA

THE PAST decade has seen the operational flood forecasting community increasingly using Hydrological Ensemble Prediction Systems (HEPS) for their forecasts. Many research studies over the past decade have shown that HEPS-based forecasts add value and can increase warning lead times. However, despite this, at present only a few flood forecasting centres around the world implement HEPS flood forecasting systems operationally (for a summary see *Cloke & Pappenberger, 2009*). There are many reasons for this, including a range of scientific, technical and cultural issues. For example, HEPS must receive and process large amounts of data generated by medium-range Ensemble Prediction System (EPS) weather forecasts (*Thielen et al., 2008; Zappa et al., 2008*). Furthermore, the computational burden of computing the flood forecasts themselves is also significant, as are the difficulties in understanding how best to base flood warning decisions on probabilistic forecasts.

Recent progress in early flood warning and system development was reviewed at the 4th Annual Workshop of European Flood Alert System (EFAS) held at ECMWF – see Box A.

In this communication, six European HEPS-based flood forecasting systems are briefly reviewed to encourage the further operational uptake of HEPS within the operational flood forecasting community. The excellent set of studies which demonstrate the potential for improving forecasts are not repeated here (see a review in *Cloke & Pappenberger, 2009*). Instead, this work concentrates on discussing how the six HEPS moved from research to operational status and describing current flood forecasting practice based on these HEPS.

AFFILIATIONS

Hannah Cloke, Sébastien Nobert: Department of Geography, King's College London, UK

Jutta Thielen, Peter Salamon: European Commission Joint Research Centre, Ispra, Italy

Florian Pappenberger, Roberto Buizza: ECMWF, Reading, UK

Gábor Bálint: VITUKI, Budapest, Hungary

Cristina Edlund: SMHI, Norrköping, Sweden

Ari Koistinen: SYKE, Helsinki, Finland

Céline de Saint-Aubin, Christian Viel: SCHAPI, Toulouse, France

Erik Sprokkereef: Rijkswaterstaat, Lelystad, The Netherlands

From research to operational implementation of HEPS in Europe

In order to develop a more complete, probabilistic approach to hydrological prediction in their systems, the institutions represented in Table 1 mostly started using the ECMWF EPS between 1999 and 2000, which is about 10 years after the launch of operational EPS in meteorology. For four of these institutions, EFAS (European Commission), Rijkswaterstaat (The Netherlands), SMHI (Sweden) and VITUKI (Hungary), work with probabilistic flood forecasting began through participation in the EU FP5 research project 'European Flood Forecasting System' (EFFS) (*de Roo et al., 2003*). Some National Meteorological Services also instigated ideas about probabilistic-based hydrological forecasts in their national institutions (e.g. SYKE in Finland, SMHI in Sweden and SCHAPI in France). Knowledge exchange within the European flood forecasting community helped foster the development of HEPS: for example, the EFAS project contributed to the introduction of

4th Annual Workshop of EFAS (European Flood Alert System), 28–29 January 2009, held at ECMWF

A

The workshop provided a forum for 43 developers and operational forecasters to discuss various topics including:

- ◆ The performance of EFAS and the national forecasting systems during flood events in 2008.
 - ◆ Progress achieved in 2008 in terms of the EFAS development and planned system improvement.
 - ◆ Research findings related to skill and post-processing of hydrological ensemble forecasting.
 - ◆ Status of data collection systems in support of EFAS.
- Also there was a training session led by ECMWF and EFAS staff on communication of probabilities and the EFAS Information System.

Presentations from the workshop are available from:

<http://www.ecmwf.int/newsevents/meetings/workshops/2009/EFAS/presentations>

More information on EFAS can be found in Thielen et al., 2009, *Hydrology and Earth System Sciences*, 13, 125–140 and at: <http://floods.jrc.ec.europa.eu>

During the workshop, alongside information on EFAS, five national institutions responsible for flood forecasting from Finland, Sweden, The Netherlands, Hungary and France provided an overview of the implementation of HEPS in their national operational flood forecasting chain. More details about these six institutions are given in Table 1.

Country	Hydro-meteorological/ flood forecasting institution	HEPS inputs	Description of HEPS	
Europe	European Flood Alert System of the European Commission, Joint Research Centre (EFAS)	ECMWF EPS and COSMO-LEPS	European Flood Alert System (EFAS) with Lisflood hydrological model	
Hungary	Water Resources Research Centre (VITUKI)	ECMWF EPS, NWS-NCEP	National Hydrological Forecasting System (NHFS) with several conceptual hydrological model components.	
Sweden	Swedish Meteorological and Hydrological Institute (SMHI)	ECMWF EPS	Hydrologiska Byråns Vattenbalansavdelning Sweden (HBVSv) with HBV hydrological model	
Finland	Finnish Hydrological Service (SYKE)	ECMWF EPS	Watershed simulation and forecasting system (WSFS) with hydrological model of conceptual HBV style	
The Netherlands	Rijkswaterstaat	ECMWF EPS and COSMO-LEPS	Flood Early Warning System (FEWS NL) with hydrological model HBV and routing model SOBEK	
France	SCHAPI (French Hydrometeorological and Flood Forecasting Service)	ECMWF EPS and Arpege EPS	SAFRAN-ISBA-MODCOU (SIM) with land surface model ISBA and hydrogeological model MODCOU	
	Pre-processing	Post-processing	Research on HEPS began in...	Operational?
Europe	Height correction of temperature; precipitation correction using ECMWF re-forecasts (in research phase)	ARMAX (in research phase)	1999	Yes, 'pre-operational' since 2005
Hungary	Global kriging utilizing regional elevation dependents of meteorological elements	–	2000	Yes, but only for emergency situations.
Sweden	Statistical downscaling according to sub-basins	–	2001/2	Yes, since 2004
Finland	Height correction on temperature and precipitation	Gaussian adjustment for real time hydrological maps	2000	Yes, since 2000 for 10 day EPS
The Netherlands	–	–	1999	No, but anticipated by end of 2009
France	Statistical and dynamical downscaling	–	2006	No, but in test phase since 2008

Table 1 From research to operational implementation: six examples of flood forecasting systems in Europe that use ECMWF EPS weather forecast inputs. For references to the individual forecast systems see *Cloke & Pappenberger (2009)*.

EPS-based flood forecasting to SCHAPI from 2005 onwards, shortly after the SCHAPI was founded.

At the time of writing (July 2009), the situation is as follows.

- ◆ Only SMHI and SYKE are routinely using HEPS for operational flood forecasts, including decision makers interacting with the forecasts.
- ◆ EFAS is currently running an HEPS in a pre-operational mode and disseminates results to the flood forecasting expert end-users in European National Hydrological Institutions.
- ◆ Rijkswaterstaat, SCHAPI and VITUKI are still at a more experimental stage.

With the exception of SYKE, which implemented an HEPS without a formal preliminary research phase, the institutions took between 4–8 years before starting to use an HEPS for operational, or at least pre-operational, activities. One major reason for this was that SYKE did not need any significant additional IT and personnel investment to implement EPS-based forecasts and thus could quickly move to an operational phase. SMHI, which also started to use their HEPS relatively quickly, was also able to rely on existing hardware. For all other institutions the setting up an HEPS represented a considerable IT investment due to the heavy computational load and disk storage requirements. However, the benefits of implementing

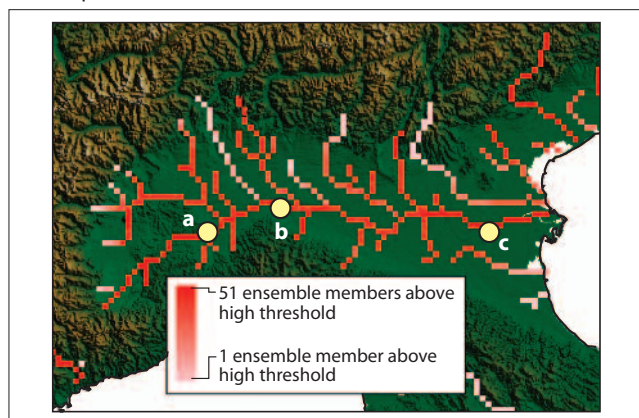
HEPS-based forecasts were seen to be worth this investment.

All the institutions listed in Table 1 use the ECMWF EPS as input to their HEPS, but almost all use these forecasts at a resolution of about 80 km, even though higher-resolution EPS forecasts (at ~50 km) have been available since September 2007. Reasons for this include the increased downloading time of the higher resolution data to the local IT environment, the increased disk storage requirements, and the fact that using EPS data at higher resolution would introduce a discontinuity in the data time series.

Some HEPS use not only the ECMWF-EPS, but also higher-resolution, limited area EPS weather forecasts (which use the ECMWF EPS as initial and boundary conditions) as input to their HEPS: in addition EFAS, Rijkswaterstaat and VITUKI incorporate COSMO-LEPS (the Limited Area Ensemble Prediction System developed within the COSMO consortium to improve the short-to-medium range forecast of extreme and localised weather events). These, higher-resolution LEPS (Limited-area Ensemble Prediction System) weather forecasts are considered to be more suitable and of higher quality for shorter forecasting times.

It is worth mentioning two other areas of research and development. SYKE has started developing and testing the

a Example from EFAS



b Example from SMHI

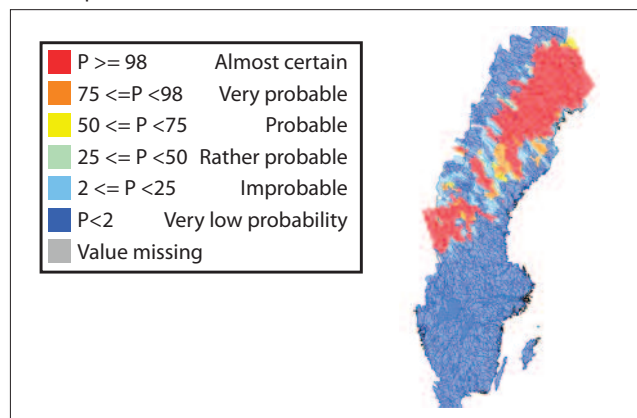


Figure 1 Example of flood probability maps from (a) EFAS showing the combined flood probability of exceeding the EFAS high flood alert from 3–10 days in advance for river pixels only from a forecast from 28 April 2008 and (b) SMHI showing the probability of exceeding the national flood level 1 which corresponds to a 2–10 year return period for May 2008. In both examples the flood threshold levels correspond roughly to return periods of 210 years.

value of HEPS forecasts on a monthly and a seasonal time scale for use in water management, while VITUKI has been assessing the value of a multi-model approach to hydrological probabilistic prediction by incorporating information from the NCEP (National Centers for Environmental Prediction) EPS in addition to the ECMWF EPS. Multi-model EPS are thought to provide higher reliability in the forecasts than single EPS, but more detailed exploitation of the multi EPS THORPEX-TIGGE archive for hydrological applications is needed to provide a better quantitative assessment of such added value for probabilistic flood forecasting (see Pappenberger et al., 2008 and He et al., 2009).

Visualisation of probabilistic results

Broadly speaking, there are two essential types of visualization used by the six institutions listed in Table 1:

- ◆ Spatial overviews in the form of maps – see Figure 1.
- ◆ Time series evolution at points – see Figure 2.

The examples in Figures 1 and 2 illustrate that visualizing probabilistic results effectively demands a strategy involving combinations of colours, numerical information and statistical plots, but that there are a range of useful ways of achieving this.

Spatial overview maps

Spatial overview maps are produced by EFAS and SMHI. EFAS produces maps with a combined flood probability value for each river pixel in the map. This value is calculated from flood models which use the full set of 51 members from the ECMWF EPS and 2 weighted runs based on the single, high-resolution forecasts from ECMWF and the German Weather Service (DWD) (Figure 1a). The values shown represent the probability of exceeding two flood threshold levels (e.g. high alert level and severe alert level) which have been previously calculated for every pixel in the map. The information is published on a password protected website for the flood forecasting experts of the EFAS partner network. SMHI publishes similar information (based on HEPS only) but based on statistical calculations on sub-catchment level (Figure 1b) and for three flood threshold levels, which correspond to the national warning levels for hydrology. For ease of access,

the maps are published for the civil protection services in the provinces on a public website, but the pages are hidden and thus the link must be known by the end-users before it can be accessed. Therefore this measure ensures that the access to the data are fast but that it can only viewed by experts that have previously been trained on the product.

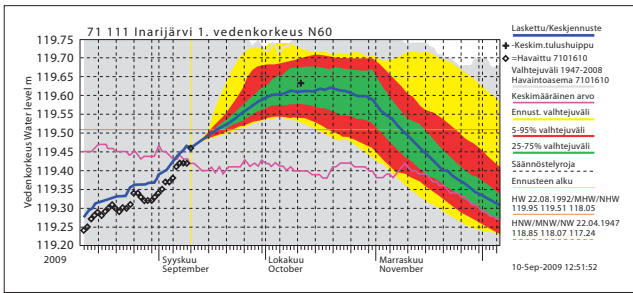
Time series information

All institutions visualize river level time series information, usually summarised as either percentiles or quantiles of the ensemble flood forecast members. Typical intervals are minimum/maximum, 25%, 50% and 75%. In some cases the probabilities are expressed as coloured shaded areas (Figure 2a) or as lines (Figure 2b). Critical thresholds are plotted as lines (Figure 2b) or shaded areas (Figure 2c). All representations include the median. Usually continuous line diagrams are used, with SCHAPI presenting results also as an ensemble of individual hydrographs (spaghetti plot) (Figure 2d).

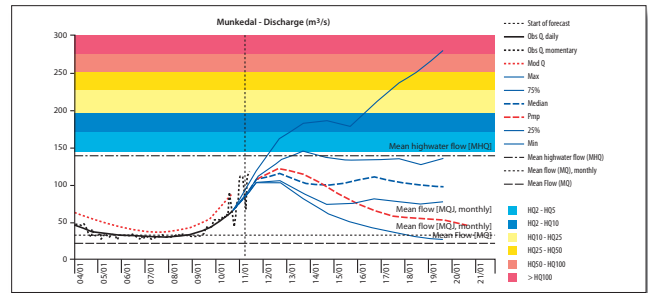
EFAS shows box-plot diagrams summarizing the EPS results in daily information of quantiles, but also shows in the same diagram the results based on the higher-resolution deterministic forecasts (Figure 2e). Through a different representation Rijkswaterstaat can actually visualize results from multiple EPS and poor-man ensembles in one complex diagram, but without losing clarity of information (Figure 2f).

Visualizing information as threshold exceedance has the advantage that the consistency between different forecasts is also visually represented at a glance. For example, Figure 2g clearly shows that all flood forecasts (based on DWD and ECMWF single high-resolution forecasts as well as on the ECMWF-EPS and the COSMO-LEPS) predict the exceedance of the EFAS high flood threshold for day 2 (2 April). The EFAS high flood alert threshold (HAL) is indicated by the red colour, the EFAS severe alert threshold (SAL) by purple. The numbers in the boxes represent the number of EPS members exceeding the corresponding EFAS flood threshold. In this case none of the ensemble members predict the exceedance of the severe alert level (SAL). The consistency between multiple forecasts can be a useful criterion for decision making.

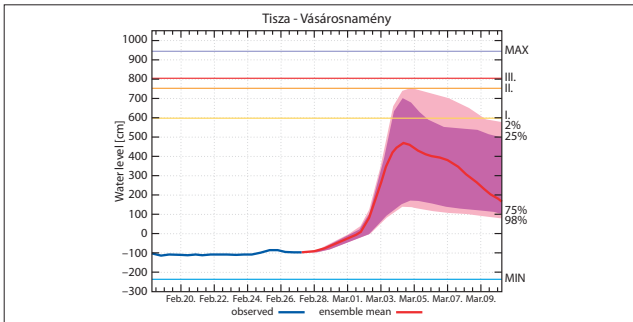
a Example from SYKE



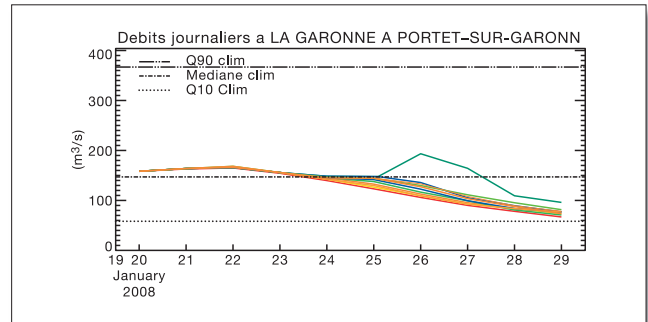
b Example from SMHI



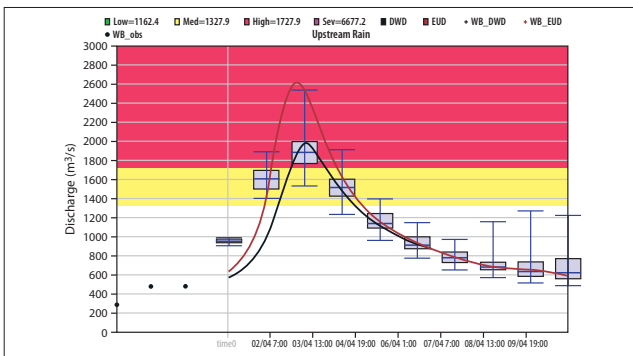
c Example from VITUKI



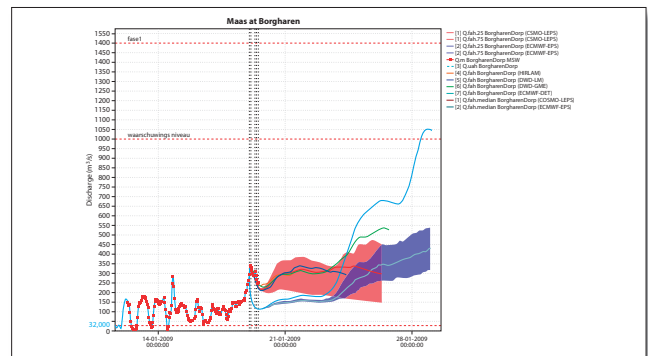
d Example from SCHAPI



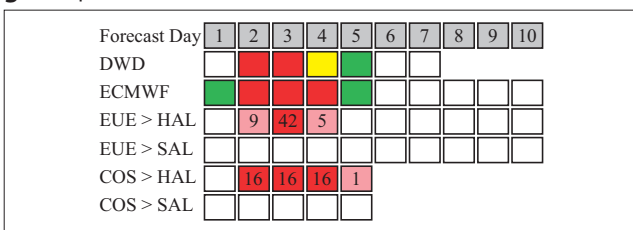
e Example from EFAS



f Example from Rijkswaterstaat



g Example from EFAS



h Example from VITUKI

River	Station	2008.03.01 6:00	2008.03.01 18:00	2008.03.02 6:00	2008.03.02 18:00	2008.03.03 6:00	2008.03.03 18:00	2008.03.04 6:00
Túr	Garbóc	16	53	135	230	295	331	352
Bodrog	Bodrogszerdahely	355	376	439	535	617	663	685
	Felsőberecki	268	288	346	425	484	524	547
	Sárospatak	281	294	335	402	458	496	512
Fekete Körös	Tenkefürdő	129	163	302	408	436	415	361
	Talpas	145	162	305	593	703	736	721
	Nagyzerénd	136	146	192	322	511	693	781
	Ant	75	94	143	264	411	565	663

Figure 2 Examples of time series information at particular locations from various flood forecasting institutions

The analysis of two years of EFAS forecasts by *Bartholmes et al.* (2009) suggested that taking into account persistence in the forecasts can reduce the number of false alarms in early flood warning. Consequently the persistence of forecasts from one forecasting day to another is also represented by some systems (not shown here).

VITUKI has opted for a similar representation but instead of showing results of different forecasts in one diagram, the exceedance of thresholds at different locations are shown. The stations are clustered by river basin and listed by upstream position (Figure 2h).

Verification of probabilistic flood forecasts

Verification of flood forecasts is an important issue for establishing trust in, and the value of, an operational system, and this becomes especially important in probabilistic flood forecasting systems. However this has proved to be difficult for extreme events such as floods. Skill scores for 'normal' conditions are computed using a long time series or a large number of cases. They have low uncertainty, are statistically sound and reflect long-term forecast performance. However, a statistically sound evaluation of extreme flood events (e.g. return periods of once every 50 to 100 years) is practically

impossible to achieve, since there will probably never be enough events to verify the probability distributions. What is important is that a transparent evaluation is carried out on the longest time series of forecasts available.

For many reasons, flood forecasting centres tend not to publish their skill scores (e.g. hit rates, flood predicted correctly, and false alarm rates, flood predicted when no flood happened) on their website, neither in a qualitative nor quantitative form. However, practice is beginning to change. For example, since the beginning of 2008, EFAS has published a monthly qualitative summary of their flood alerts listing to whom the alerts were sent and if flooding or high water was reported, and skill score calculation and publication is currently being implemented. With new products continuously being added to forecasting systems, skill assessment is difficult and until a sufficient number of time series are available, these must be evaluated visually and by simple scoring.

For the five national HEPS presented in Table 1, a range of visual comparison and skill score comparisons are currently used internally. For example, VITUKI assesses skill by comparing the Nash Sutcliffe values of their HEPS with the naive forecast. Also SMHI evaluates forecasts using several statistical measures including both threshold and percentile based scores (see *Olsson & Lindstrom, 2008*). Other organisations complement verifications by benchmarking their forecasts, for example, the forecasts issued by SHAPI is in the process of being compared to the EFAS system.

Communication of probabilistic flood forecasts

Interpreting probabilistic forecasts is not straightforward. Whilst single forecasts provide an easier-to-interpret (yes-or-no) answer for end-users, probabilistic forecasts by their nature shift responsibility towards the end-user for the interpretation of results for decision making. For example, what is the minimum probability value when it makes sense to issue a warning for a severe flood event? Since the minimum probability is linked to the cost/loss ratio of taking a protective action (see the example and discussion in *Buizza et al., 2007*), the end-users are the only ones with the information (i.e. the cost/loss ratios) to be able to define it. Are these probabilities thresholds the same for medium and severe events? For end-users that are used to having forecasts that predict an exact amount of flooding at a particular point in time, how can they begin to use probabilistic information instead?

Increased communication between the developers of probabilistic systems and the end-users, and more targeted, end-user training can help in identifying the correct answer to these questions. End-users need to become familiar with probabilistic forecast products. In particular, they need to understand exactly what probabilistic forecasts are (and what they are not), and in what ways they are more useful than single, yes-or-no forecasts (such as better potential for early warning and capturing uncertainty). Commonly used training approaches used by EFAS and other flood forecasting centres range from lectures and games in an artificial setting to training in realistic case studies and in situ training. For example, EFAS trains end-users using case studies of real flood events from Europe and thus allows a realistic

participatory learning approach. In these case studies, participants have to undertake role playing where they must make decisions and issue warnings to civil protection based on a replay of real flood forecasts. SHAPI communicates by daily briefings with regional forecasting centers. SMHI has a strong communication network with their end-users and has chosen to organize training on HEPS flood forecasts within the local authorities in Sweden. This is likely to be very important if probabilistic forecasting is to be adopted by such end-users.

Outlook for probabilistic flood forecasts

Ensemble flood forecasting has emerged as the state of the art in medium-range flood forecasting over the last five to six years. Europe is at the forefront of exploiting a probabilistic approach in flood forecasting. The evidence points to more and more operational flood forecasting centres looking to use the ECMWF-EPS and/or higher-resolution, limited area ensemble systems (e.g. COSMO-LEPS) in their HEPS to increase the early warning capacity of their systems. While achievements in implementing HEPS are significant and should not be downplayed, the authors of this communication think that more research is needed to further improve the current systems, and that further effort should be put into visualizing, verifying, developing user-specific applications for, and communicating the value of probabilistic flood forecasts.

FURTHER READING

Bartholmes, J., J. Thielen, M. Ramos & S. Gentilini, 2009:

The European flood alert system EFAS – Part 2: statistical skill assessment of probabilistic and deterministic operational forecasts. *Hydrol. Earth System Sci.*, **13**, 141–153.

Buizza, R. & 26 others, 2007: EURORISK/PREVIEW report on the technical quality, functional quality and forecast value of meteorological and hydrological forecasts. *ECMWF Tech. Memo. No. 516*.

Cloke, H. & F. Pappenberger, 2009: Ensemble Flood Forecasting: A Review. *J. Hydrol.*, doi:10.1016/j.jhydrol.2009.06.005, **375**, 613–626. Also *ECMWF Tech. Memo. No. 574*.

de Roo, A. P. J. & 20 others, 2003: Development of a European flood forecasting system. *Int. J. River Basin Management*, **1**, 49–59.

He, Y., F. Wetterhall, H.L. Cloke, F. Pappenberger, M. Wilson, J. Freer & G. McGregor, 2009: Tracking the uncertainty in flood alerts driven by grand ensemble weather predictions. *Meteorol. Appl.*, **16**, 91–101.

Olsson, J. & G. Lindstrom, 2008: Evaluation and calibration of operational hydrological ensemble forecasts in Sweden. *J. Hydrol.*, **350**, 14–24.

Pappenberger, F., J. Bartholmes, J. Thielen, H.L. Cloke, A. de Roo & R. Buizza, 2008: New dimensions in early flood warning across the globe using GRAND ensembles. *Geophys. Res. Lett.*, **35**, L10404 doi:10.1029/2008GL033837.

Thielen, J., J. Schaake, R. Hartman & R. Buizza, 2008: Aims, challenges and progress of the Hydrological Ensemble Prediction Experiment (HEPEX) following the third HEPEX workshop held in Stresa 27 to 29 June 2007. *Atmos. Sci. Lett.*, **9**, 29–35.

Zappa, M. & 15 others, 2008: MAP D-PHASE: Real-time demonstration of hydrological ensemble prediction systems. *Atmos. Sci. Lett.*, **2**: 80–87, doi: 10.1002/asl.183.

An experiment with a 46-day Ensemble Prediction System

FRÉDÉRIC VITART, FRANCO MOLteni

THE ECMWF monthly forecasting system has been operational since October 2004. It was originally based on 32-day integrations of a coupled ocean-atmosphere system that were produced once a week with an atmospheric horizontal resolution of T159. Initially this system was run separately from the Ensemble Prediction System (EPS) and the seasonal forecasting system. Since March 2008, the monthly forecasting system has been merged with the EPS.

The aim of this article is to describe an investigation into the possibility of extending the length of the mid-month monthly forecast from 32 days to 46 days so that it fully covers the next calendar month. It was recognised that this approach might produce a more accurate and reliable outlook for the second calendar month than the ECMWF seasonal forecasting system for the following reasons.

- ◆ More up-to date forecasts (the ECMWF seasonal forecasts are issued 15 days behind real-time, whereas the monthly forecasts are issued the same day as the forecast starting date).
- ◆ A more up-to-date model cycle - the seasonal forecasting system uses a frozen version of ECMWF's Integrated Forecast System (IFS).
- ◆ Higher resolution of the atmospheric model.

Here, the forecast skill of the 46-day EPS will be compared to the skill of the current seasonal forecasting known as System 3 (Anderson *et al.*, 2007).

Experimental setup

A series of 46-day hindcasts has been performed for the 20-year period from 1989 to 2007. The hindcasts start on the 15th of each month and are 46-days long to fully cover the next calendar month. The 15th of the month was chosen because it is the date the seasonal forecasts from System 3 are disseminated. For each starting date, the hindcasts consist of an ensemble of 15 members: a control and 14 perturbed forecasts. In this investigation, only the first 10 perturbed forecasts will be considered to be consistent with the System 3 hindcasts.

The version of IFS used in this experiment is Cy32r3, which was operational from November 2007 until June 2008. The configuration of the hindcasts is the same as the one used for operational monthly forecasts at ECMWF, except for the length of the forecasts (46 days instead of 32 days for the operational monthly forecasts). In this configuration, the IFS is first integrated for 10 days with a resolution of T399 (about 50 km resolution) and 62 vertical levels. At day 10, the horizontal resolution is lowered to T255 (about 80 km resolution) till the

end of the forecast. During the first 10 days, the IFS is forced by persisted SST anomalies. After day 10, the IFS is coupled to the HOPE oceanic model every 3 hours. The initial conditions are taken from the ERA-40 reanalysis till 2001 and ECMWF operational analysis thereafter. The ensemble perturbations are produced in the same way as in the operational monthly forecasts. More details about the model configuration can be found in Vitart *et al.* (2008).

In this investigation, we will compare the 46-day EPS forecasts of the next calendar month with the seasonal forecast from System 3 starting on the 1st of the month but available on the 15th of the month (same day as the monthly hindcasts). For instance for the month of June 2007, we compare the month 2 of the seasonal forecast starting on 1 June 2007 (available on the 15 June 2007) to the EPS forecasts for days 16–46 starting on 15 June 2007.

Probabilistic scores

We now compare the probabilistic scores for month 2 of System 3 with those obtained with the 46-day EPS. Figure 1 shows the relative operating characteristic (ROC) diagrams of the probability that the 2-metre temperature averaged over the next calendar month is in the upper tercile for the northern extratropics (Figure 1a) and the tropics (Figure 1b) in winter. According to Figure 1, the EPS forecasts are more skilful for predicting 2-metre temperature probabilities than month 2 of System 3. The difference is statistically significant within the 5% level of confidence according to the Wilcoxon-Mann-Whitney test. The 46-day EPS forecast also provides better scores than month 2 of System 3 for other variables such as precipitation and mean-sea-level pressure. Similar results are found for the other seasons.

Another way of assessing the skill of probabilistic forecasts is to use reliability diagrams (observed frequency as a function of forecast probability). Figure 2 shows the reliability diagram of the probability of the 2-metre temperature being in the upper tercile for the 46-day EPS forecasts and month 2 of System 3 over the northern extratropics. These results show that the 46-day EPS forecasts are more reliable than month 2 of System 3.

Increasing the horizontal resolution from T159 to T255 had some positive impact on the probabilistic scores for the extended EPS forecasts (Vitart *et al.*, 2008), but the improvement was significantly lower than the difference displayed in Figures 1 and 2. Therefore most of the difference in skill between the 46-day EPS and System 3 is likely due to the EPS forecasts benefiting from more recent initial conditions and also from a more recent model cycle. It is not clear at this point which of those two factors makes the most important contribution on the probabilistic scores.

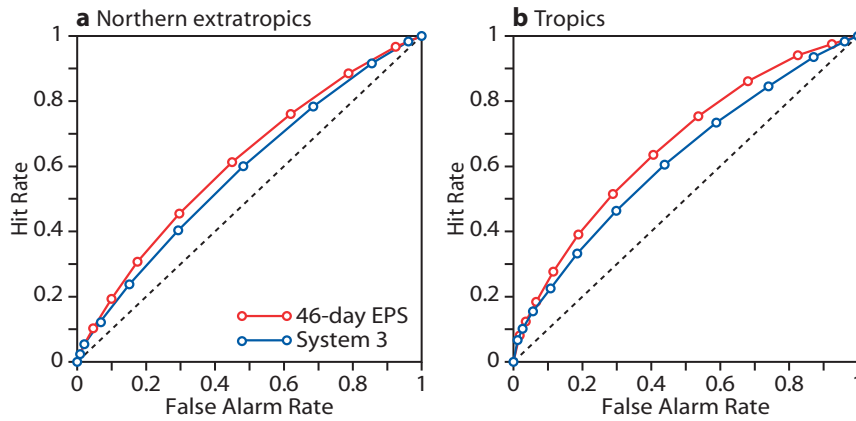


Figure 1 ROC diagrams of the probability that the 2-metre temperature is in the upper tercile for (a) northern extratropics and (b) tropics for the next calendar month for the 46-day EPS and month 2 of System 3 for the period December to February. Only land points have been scored. The further the curve is towards the upper left-hand corner the more skilful the forecast.

It is possible that the skill of the 46-day EPS to predict 2-metre temperature anomalies of the next calendar month comes from day 16–30 forecasts and that there is no skill beyond day 30. To test this hypothesis, the anomalies of day 16–30 have been persisted to predict the 2-metre temperature anomalies of day 31–45. Results (not shown) indicate that persisting day 16–30 anomalies provides significantly less reliable probabilistic forecasts than day 31–45 of the EPS forecasts. This indicates that extending the EPS forecasts until day 46 is useful.

Two examples concerning extreme events

We will now discuss two specific cases of extreme events over Europe: the heatwave over Europe in the summer of 2003 and the unusually wet summer of 2007 in England.

Heatwave over Europe in the summer of 2003

The heatwave in the summer of 2003 killed about 35,000 people in Europe, and is therefore a particularly important case for monthly forecasting. Here we focus on August 2003, when the 2-metre temperature monthly mean anomalies were the highest and exceeded 4°C. For this specific case, the size of the 46-day EPS hindcasts starting on 15 July has been increased to cover the 30-year period from 1978 to 2007.

It is interesting to consider the ensemble distributions of the seasonal forecasts from System 3 starting on 1 July and the 46-day EPS forecasts starting on 15 July. Figure 3 shows the interannual variability of the ensemble mean, 25% and 75% values, and maximum and minimum of the ensemble distributions. In the seasonal forecast starting on the 1 July (Figure 3a), August 2003 does not stand out as being an exceptional month. However, in the 46-day EPS forecast (Figure 3b), August 2003 is predicted as being exceptionally warm. It is indeed predicted as being the warmest month of the 30-year period, although the predicted anomalies are still lower than observed. This suggests that the 46-day EPS could have been of value as an early warning for this heatwave over Europe.

To assess the impact of the horizontal atmospheric resolution on the 46-day EPS forecast, an additional EPS forecast has been produced with the same model version, but with a T159 resolution (same resolution as System 3). In this set of low-resolution EPS forecasts, August 2003 is no longer predicted as the warmest month of the 30-year period. This

suggests that part of the improvements in the 2-metre temperature forecasts for August 2003 from the 46-day EPS compared to that from System 3 (Figure 3) is due to the higher resolution of the EPS.

Wet summer of 2007 in England

July 2007 was exceptionally wet over England, with record precipitation that led to significant flooding over Southwest England, particularly during the week of 16–22 July 2007. On the other hand, this month was particularly dry and hot over most of southern Europe, mostly in Southeast Europe as illustrated by the reanalysis (Figure 4a).

Figure 4b shows the probability of a positive anomaly of precipitation over Europe in the 46-day EPS forecasts starting on 15 June 2007. The anomalies have been calculated relative to the 1989–2006 model climatology. These results show that the 46-day EPS forecasts starting on 15 June were successful at predicting a high probability of a wetter than

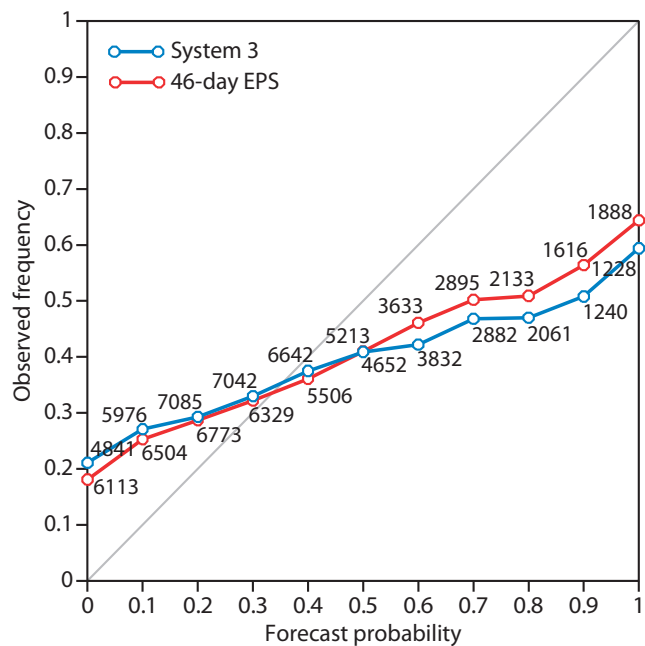


Figure 2 Reliability diagram of the probability that 2-metre temperature over the northern extratropics is in the upper tercile for the next calendar month for the 46-day EPS and month 2 of System 3 for the period December to February. Only land points have been scored. The closer the curve is to the diagonal the more reliable the forecast.

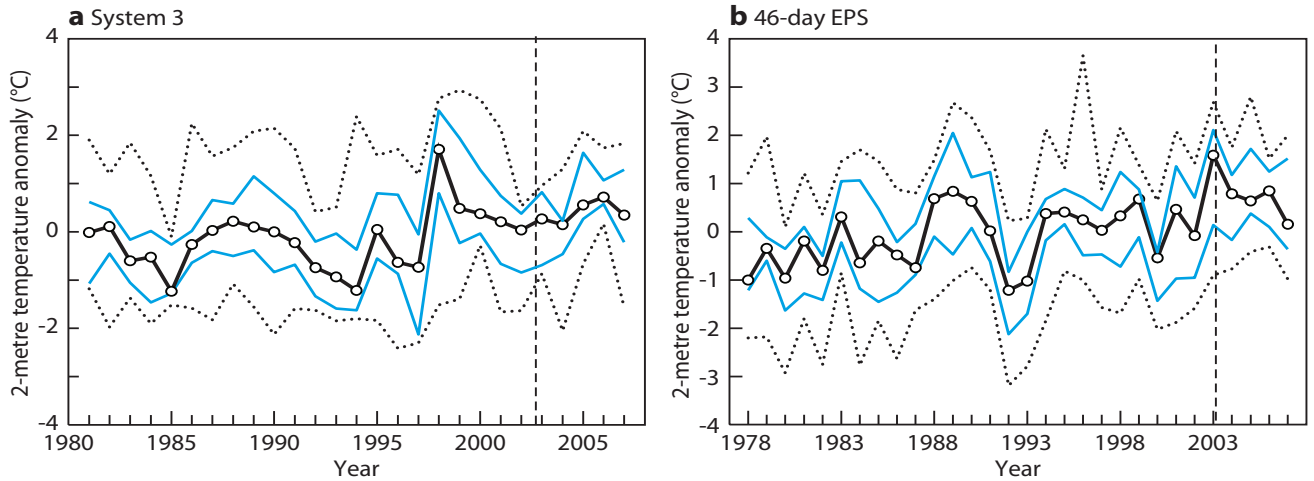


Figure 3 2-metre temperature ensemble distribution for (a) System 3 starting on 1 July and (b) 46-day EPS starting on 15 July. The solid black line represents the median. The blue line represents the 25% and 75% distributions. The black dotted lines represent the maximum and minimum of the distribution. The 2-metre temperature anomalies have been averaged over the area: 0–20°E, 40–50°N.

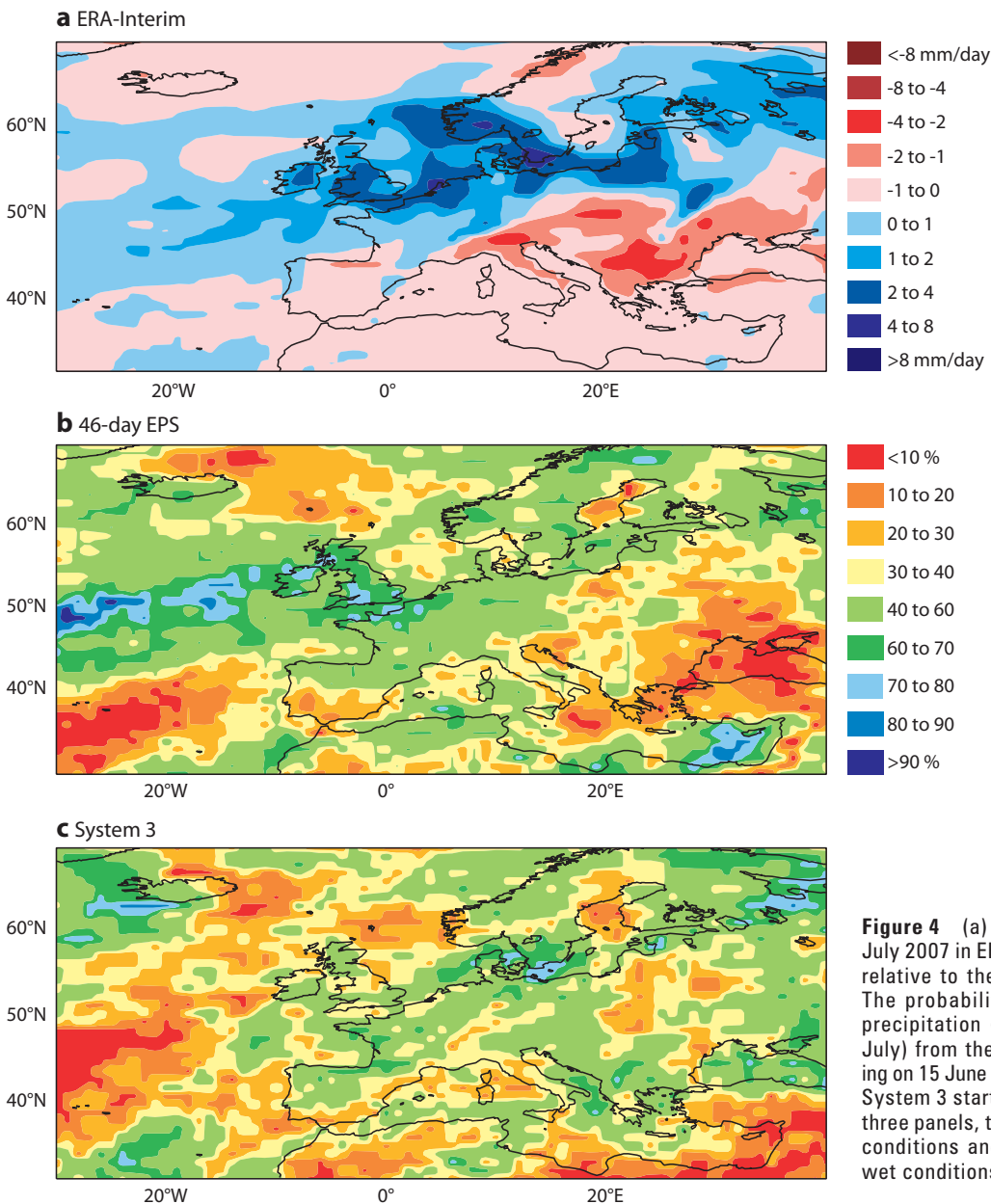


Figure 4 (a) The precipitation anomaly for July 2007 in ERA-Interim. The anomalies are relative to the period July 1989–2006. (b) The probability of a positive anomaly of precipitation (wetter than usual month of July) from the 46-day EPS forecasts starting on 15 June 2007. (c) The probabilities from System 3 starting on 1 June 2007. In all the three panels, the red contours represent dry conditions and the blue contours indicate wet conditions.

normal July 2007 over England, although the precipitation anomaly does not extend as far east as in the reanalysis (Figure 4a). The low probability of a wetter than normal July over Southeast Europe is also consistent with the reanalysis. On the other hand, the System 3 hindcasts starting on 1 June 2007 (Figure 4c) do not predict a higher probability than normal of a wet month over England. The probability of a dry July over Southeast Europe is also much smaller than in the 46-day EPS forecast. This result suggests that the 46-day EPS forecast would have provided a much better warning for those severe events than the System 3 forecast starting on 1 June.

Atlantic hurricanes

The prediction of extreme events, such as hurricanes, is likely to benefit from a higher horizontal resolution. It is therefore expected that the higher resolution of 46-day EPS forecasts should produce more accurate hurricane forecasts than month 2 of System 3.

Figure 5 shows the climatological density of tropical storm tracks taken from observations (panel a), 46-day EPS forecasts for days 16–45 (panel b) and forecast for months 2 and 1 from System 3 (panels c and d). The 46-day EPS and System 3 forecasts tend to produce too many storms in the Atlantic at those extended time ranges. The patterns of the tropical storm density tracks are more realistic in the 46-day EPS than in System 3: in the 46-day EPS climatology, there is significant tropical cyclone activity in the mid-Atlantic and in the Gulf of Mexico, whereas most of the tropical cyclone

activity in System 3 is concentrated between 10° and 20°N in the Atlantic. This is the main area where easterly waves develop into tropical storms. This difference in model climatology is not due to the 46-day EPS forecasts having a shorter lead time than month 2 of System 3: month 1 of System 3 shows a similar climatology to month 2 (compare Figure 5d with Figure 5c).

Sensitivity experiments have been performed to show that the difference in tropical cyclone climatology between System 3 and the 46-day EPS is mostly due the difference in model cycles.

The 46-day EPS shows a higher skill at predicting the interannual variability of the number of Atlantic hurricanes in individual months (Table 1) than not only month 2 of System 3, but also month 1 of System 3 that starts 15 days after the 46-day EPS. This improvement in the prediction of hurricane is essentially due to the higher resolution of the 46-day EPS compared to System 3. At the System 3 resolution (T159), the number of hurricanes simulated over a month by the model is too low to produce meaningful statistics. However, at T255, the number of hurricanes, although still lower than observed, is large enough to produce a realistic interannual variability.

Early monsoon rainfall prediction

The prediction of Indian rainfall in June represents a particularly difficult challenge. During the month of June, the level of Indian rainfall is strongly linked to the onset of the monsoon, which is usually difficult to predict more than

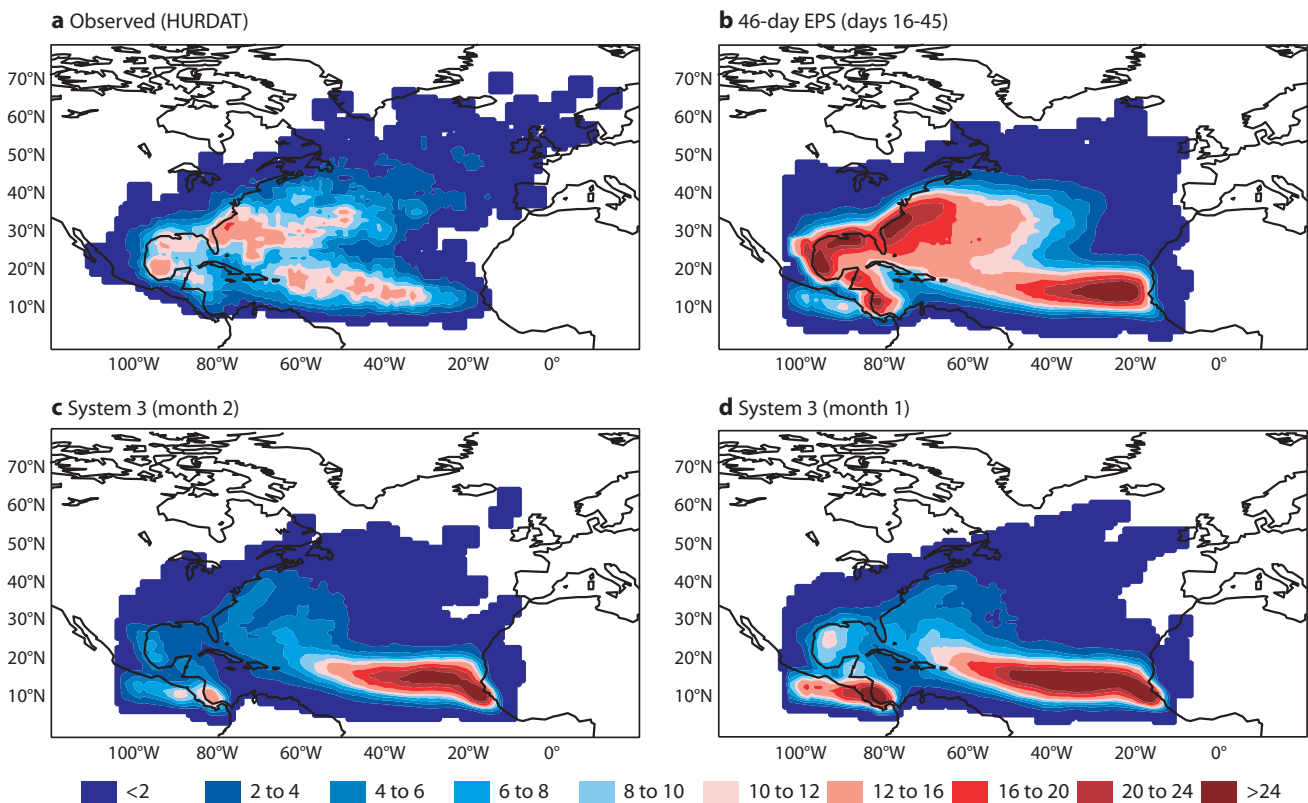


Figure 5 Density of tropical storms ($\times 1000$) from (a) Atlantic basin hurricane database (HURDAT), (b) days 16–45 of the 46-day EPS forecasts, (c) month 2 of System 3 and (d) month 1 of System 3 for August to September 1989–2007. The density of tropical storms is defined here as the number of tropical storms per day passing within 200 km.

Forecast system	August	September	October
46-day EPS	0.77	0.37	0.69
System 3 – Month 1	0.31	0.33	0.18
System 3 – Month 2	-0.03	0.23	0.18

Table 1 Correlation between the interannual variability of hurricanes for the period 1989–2007 from an Atlantic basin hurricane database (HURDAT) and 46-day EPS forecasts starting on the 15th of the previous month (forecast range: days 16–45), month 1 of the seasonal forecast starting the 1st of the month and month 2 of the seasonal forecast starting the 1st of the previous month for August, September and October.

two weeks in advance. The skill of System 3 to predict monsoon rainfall has been evaluated by *Molteni et al.* (2008). They found that this dynamical seasonal forecasting system displays some skill at predicting monthly-mean precipitation over India after July, but has surprisingly low skill at predicting the June precipitation over India.

Table 2 shows that the correlation between the interannual variability of June precipitation over India predicted by System 3 starting on 1 May (time range: month 2) is only 0.40 for the period 1989–2007. On the other hand the 46-day EPS starting on 15 May has a correlation of 0.62 that is significantly higher than that for System 3. The root-mean-square error is also significantly lower in the 46-day EPS than with System 3. Interestingly, the 46-day EPS also outperforms the forecast from System 3 starting on 1 June (15 days later than the 46-day EPS) – see Table 2. The difference, although smaller than between the 46-day EPS and System 3 starting on 1 May, is statistically significant (within the 1% level of significance using a 10,000 bootstrap re-sampling procedure). Those results are consistent with those found by *Vitart & Molteni* (2009), which used a previous version of the IFS (Cy32r2).

The fact that the 46-day EPS produces more accurate indications of early monsoon rainfall than System 3 cannot be attributed to the more up-to-date initial conditions, since they also outperform seasonal forecasts starting 15 days later. In order to establish if this improvement is due to the increased resolution, the 46-day EPS experiment was repeated but with a T159 resolution (same resolution as System 3). The scores obtained with this low atmospheric resolution were

Forecast system	Start date	Correlation	RMS error
46-day EPS	15 May	0.62	0.90
System 3– Month 2	1 May	0.40	1.15
System 3– Month 1	1 June	0.52	0.96

Table 2 Correlation and root-mean square (RMS) error between the interannual variability of June rainfall over India (only land points are used in the calculation) for 1989 to 2007 for the 46-day EPS, month 2 of System 3 starting on 1 May, and month 1 of System 3 starting on 1 June. The observed data is the 1°×1° gridded daily rainfall data from the India Meteorological Department (Rejeevan et al., 2006, *Current Science*, 91, 296–306).

very close to those obtained with System 3. This suggests that the monsoon rainfall forecasts for June benefit from the higher resolution of the 46-day EPS.

Benefits of using the 46-day EPS

In this short article, we have presented results from an experiment where the EPS forecasts have been extended to 46 days. The main conclusion is that extending EPS forecasts can lead to more accurate and reliable forecasts of the next calendar month than with the current seasonal forecasting system (System 3). It has been shown that the probabilistic scores are better with the 46-day EPS forecasts than with month 2 of System 3. In particular, the prediction of severe and extreme events like the 2003 heatwave over Europe, the wet July 2007 over England, the frequency of hurricanes and early monsoon rainfall is significantly more accurate with the 46-day EPS than with System 3.

The forecast improvements are due to different factors: the improvements in the probabilistic scores are due mostly to the more up-to-date initial conditions and model cycle. However, the forecasts of hurricane frequency or early monsoon rainfall produced by the 46-day EPS are more accurate than the System 3 forecasts starting 15 days later (month 1). For those severe events, the increase of the atmospheric resolution seems to be the main factor explaining the improvement. The benefits from a more recent IFS cycle were shown in the case of the Atlantic tropical storm climatology, which is much more realistic in the 46-day EPS than in System 3. Therefore, more up-date model cycle, more up-to-date initial conditions and higher resolution are factors which together help to produce better forecasts of the next calendar month.

At the moment no decision has been taken on the possibility to operationally extend the EPS beyond the current 32 days. In any case, such an extension should be seen as a complement to the seasonal forecast: the next version of the ECMWF seasonal forecasting system (System 4) will remain separate from the EPS. Further research will be performed to investigate the potential benefit of extending the EPS and to determine its optimal overlap with the seasonal forecasting system.

FURTHER READING

- Anderson, D., T. Stockdale, M. Balmaseda, L. Ferranti, F. Vitart, F. Molteni, F. Doblas-Reyes, K. Mogensen & A. Vidard, 2007: Development of the ECMWF seasonal forecast System 3. *ECMWF Tech. Memo. No. 503*.
- Molteni, F., F. Vitart, T. Stockdale, L. Ferranti & M. Balmaseda, 2008: Prediction of tropical rainfall with the ECMWF seasonal and monthly forecast systems. In *Proc. ECMWF Workshop on Ensemble Prediction*, 7–9 November 2007, ECMWF, Reading, UK.
- Vitart, F., R. Buizza, M. Alonso Balmaseda, G. Balsamo, J.-R. Bidlot, A. Bonet, M. Fuentes, A. Hofstadler, F. Molteni & T. Palmer, 2008: The new VAREPS-monthly forecasting system: a first step towards seamless prediction. *Q. J. R. Meteorol. Soc.*, **134**, 1789–1799.
- Vitart, F. & F. Molteni, 2009: Dynamical extended-range prediction of early monsoon rainfall over India. *Mon. Wea. Rev.*, **137**, 1480–1492.

Evaluation of AMVs derived from ECMWF model simulations

.....
**LUEDER VON BREMEN, NIELS BORMANN, STEVE WANZONG,
MARIANO HORTAL, DEBORAH SALMOND,
JEAN-NOËL THÉPAUT, PETER BAUER**
.....

IN A collaborative project between ECMWF and the Cooperative Institute for Meteorological Satellite Studies (CIMSS), Atmospheric Motion Vectors (AMVs) derived from simulated image sequences have been investigated to shed further light on the interpretation of real AMVs used for NWP. This pilot study has demonstrated the potential of the simulation framework to characterize errors in actual AMVs and identified a number of issues that require further investigation. For example, the influence of cloud evolution and thickness on biases in AMVs has been highlighted, an area that has so far received much less attention than height assignment issues.

Improving the characterization and interpretation of AMVs

AMVs are wind observations derived from image sequences obtained from geostationary or polar-orbiting satellite data. They are an established ingredient to global and regional data assimilation systems. The wind information is retrieved by tracking features such as clouds in subsequent images, assuming that the feature acts as a passive tracer of the atmospheric flow. The resulting wind vector is assigned to a pressure level, typically an estimate of the cloud top for higher-level clouds, and the cloud base for lower-level clouds. ECMWF currently assimilates AMVs from five geostationary and two polar-orbiting satellites, with data derived at EUMETSAT, NOAA/NESDIS and JMA.

Monitoring of AMVs against short-range forecast information or against collocated radiosonde observations often shows considerable biases or larger, more random deviations in certain geographical regions. Particular problem areas are slow speed biases for high-level extra-tropical AMVs, and fast biases for mid-level AMVs in the tropics. It is generally accepted that a large proportion of these biases or deviations can be attributed to the indirect measurement method of AMVs. On

the one hand, several steps in the AMV processing can introduce such errors, especially the height assignment which tends to rely on information from just a few infrared and water-vapour channels. On the other hand, the interpretation of the AMVs as single-level wind observations can also be prone to errors, for instance because the tracked motions may be more representative of a layer-wind, or because the tracked feature may not strictly be a passive tracer.

The assimilation of observations with systematic biases and geographically varying quality poses particular challenges for data assimilation. As the assimilation system assumes unbiased observations, biases need to be removed before or during the assimilation. This requires a good understanding of the biases and their origin, and an adequate model for the bias characteristics. For AMVs, modelling of biases has so far been unsuccessful, primarily owing to the indirect measurement method used in AMVs. Geographically varying quality of observations can be addressed through varying the observation error or through adequate quality control. Both require a good understanding of the sources of the errors.

Improvements in the characterization and interpretation of AMVs are therefore required for a better assimilation of AMVs in the ECMWF system. Further analysis of the origin of the errors and improvements in the interpretation of the AMVs are difficult as other correlative observations with sufficient coverage and including detailed information on winds and clouds are not usually available.

A simulation framework has now been used in a pilot study to improve our understanding of AMVs and their interpretation. Image sequences were simulated from high-resolution ECMWF forecast fields over a 6-hour period (at T2047, ~10 km spatial resolution). AMVs were subsequently derived from these images at CIMSS. The derived AMVs, in turn, were compared back to the wind field of the atmospheric model underlying the image simulations. In this framework the 'true' wind field and the position and vertical extent of the cloud or humidity features are exactly known – they are given by the values from the high-resolution ECMWF forecast fields.

The simulation provides the opportunity to characterize in detail the errors that have arisen in the AMV processing and/or arise from the assumption that clouds are near-perfect passive tracers of the ambient wind at a single level and location. The study also allows us to shed light on height assignment which has long been established as one crucial area for AMV processing. The aim is to provide further characterization of AMVs which will lead to an enhanced assimilation of the data, for instance, through improvements in the interpretation of AMVs ('observation operator'), developments for a bias correction, or revisions to the quality control. The study was based on Meteosat-8 imagery (6.2, 7.3

AFFILIATIONS

Lueder von Bremen*, Niels Bormann, Mariano Hortal,
Deborah Salmond, Jean-Noël Thépaut, Peter Bauer:

ECMWF, Reading, UK

Steve Wanzong: Cooperative Institute for Meteorological Satellite Studies (CIMSS), University of Wisconsin, Madison, USA

* Visiting Scientist at ECMWF from Carl von Ossietzky Universität Oldenburg, Germany, funded by EUMETSAT's NWP Satellite Application Facility

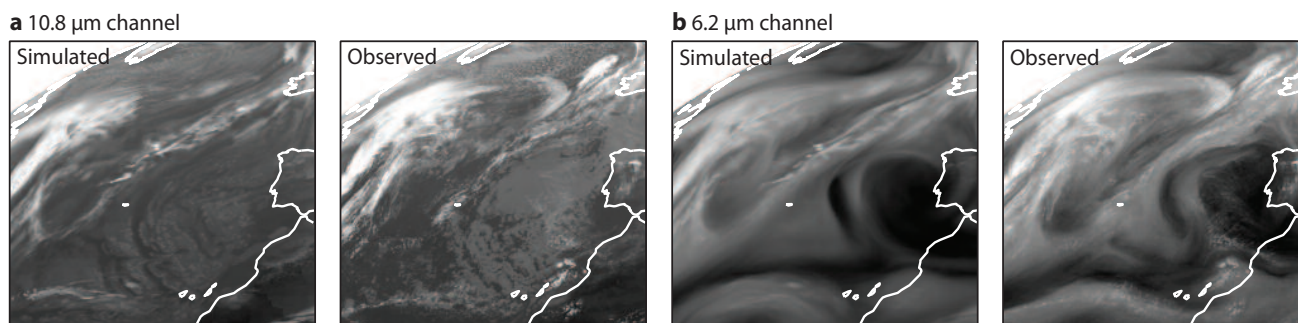


Figure 1 Detail of simulated (left) and observed Meteosat-8 (right) images for (a) infrared $10.8 \mu\text{m}$ and (b) $6.2 \mu\text{m}$ channels at 15.45 UTC on 2 January 2006.

and $10.8 \mu\text{m}$ channels), and the images were simulated every 15 minutes for clear and cloudy conditions using RTTOV-Cloud, a radiative transfer model.

An example of simulated and observed images from two channels is shown in Figure 1. For our purposes, an exact correspondence between the simulated and observed images is of secondary importance; more important is that the general structure and spatial details of the simulated images adequately resemble the observed ones. Generally speaking, this is the case – the simulated images indeed appear realistic. However, it is also clear from just this one example that there is additional small-scale structure in the real infrared image, for example around the frontal band in the upper half of the images (Figure 1a). This is not too surprising, as the model resolution that is currently possible with the Integrated Forecast System (IFS) used for this study is still significantly lower than the 3–5 km resolution of today's geostationary imagers. Also, in contrast to the infrared simulation, the simulated water-vapour image shows an under-representation of cirrus (Figure 1b). Such shortcomings in the simulation approach have to be kept in mind when interpreting the results, as the underlying assumption of using simulated imagery for the characterization of AMVs is that the simulation adequately represents reality.

The winds derivation for this study was performed by CIMSS, using an algorithm that is similar to that used by NOAA/NESDIS for the operational derivation of GOES AMVs. The processing requires as input atmospheric background information which is used in the quality control of the data as well as in the height assignment. Two AMV datasets were provided by CIMSS, one using the operational forecasts from NOGAPS (Navy Operational Global Atmospheric Prediction System) as background and one in which ECMWF model data from the 'truth' forecast was used as background information. Comparison of the two sets allows us to investigate the relative impact of the model data on the AMV product. CIMSS made winds available in two forms: before quality control ('raw') as well as quality-controlled AMVs. The latter passed a number of internal quality checks and were post-processed by a recursive filter, the so-called auto-editor.

Comparison to monitoring statistics for real AMVs

As a first step, difference statistics for the simulated AMVs against the model truth can be compared to monitoring statistics of real AMVs against a short-term forecast (first

guess). The patterns of speed biases and normalized root mean square vector differences (NRMSVD) for simulated and observed AMVs show several similarities. For example, compare the zonal mean speed bias (AMV minus 'truth') for simulated infrared AMVs before auto-editing (Figure 2a) and after auto-editing (Figure 2b) with the equivalent bias for real Meteosat-8 AMVs (Figure 2c). For the three datasets, negative speed biases prevail at high levels in the extra-tropics and positive biases at mid-levels in the tropics, especially in the simulated AMVs before quality control.

Overall, it appears that a simulation study of this type can adequately represent true observation statistics. Nevertheless, some differences exist, for instance in terms of the coverage in the vertical of water-vapour winds (not shown) or the zonal mean bias characteristics for low-level AMVs. Note, that real AMV first-guess statistics include contributions from the forecast errors, whereas for the simulations we compare AMVs to the 'truth'. Also, the real Meteosat-8 AMVs were derived with the EUMETSAT processing rather than the CIMSS processing; however, differences in monitoring characteristics for EUMETSAT and CIMSS-derived AMVs are usually reduced when CIMSS winds before auto-editing are considered (e.g. http://www.metoffice.gov.uk/research/interproj/nwpsaf/satwind_report/index.html).

Next, the influence of the atmospheric background information can be studied. This background information is used in the derivation of the winds for the initial height assignment and in complex quality control procedures. Considering the AMVs before the quality control, it was found that the influence of the background data on the height assignment has little impact on the AMV quality in our simulations. AMVs derived with the NOGAPS background compared similarly well to the truth from the forecast simulation as AMVs derived with knowledge of this truth. It appears that the height assignment has relatively small sensitivity to the background used in the processing, at least within current short-term forecast errors. This is an important finding for NWP, as it is easier to assimilate observations that are independent of short-term forecast errors.

Though the height allocation appears relatively insensitive to the background, the quality control introduces a noticeable dependence on the background information used in the processing. After the CIMSS quality control, AMVs derived and post-processed with ECMWF fields compare better with the 'true' winds than those derived and quality-controlled with

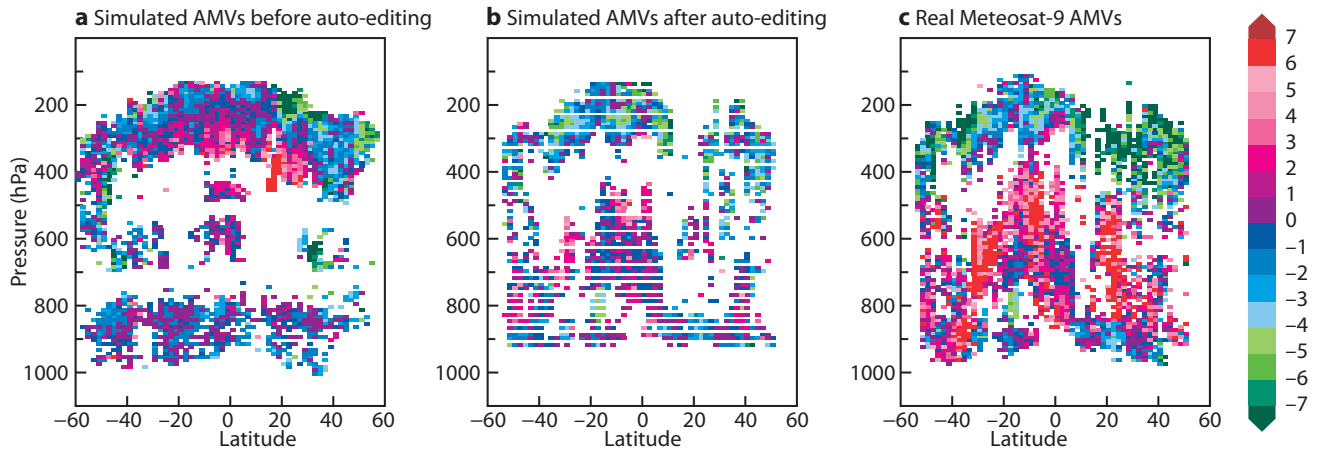


Figure 2 Zonal mean speed bias (AMV minus ‘truth’, ms^{-1}) for simulated infrared AMVs (a) before auto-editing and (b) after auto-editing derived with the NOGAPS background for 12–18 UTC on 2 January 2006 (the stripes are due to the discretization of the background data). (c) The equivalent zonal mean speed bias for real Meteosat-8 AMVs. Quality Indicator > 60% – this is a measure of the AMV’s consistency within the derived wind field. The numbers of winds used in the three sets of results are 27,504, 18,884 and 43,056.

NOGAPS fields (e.g. bias and NRMSVD for high-level cloudy water-vapour AMVs over the southern hemisphere are -1.5 ms^{-1} and 0.38 for NOGAPS AMVs, and -0.6 ms^{-1} and 0.35 for ECMWF AMVs). The ECMWF fields used represent the truth in this study, so that the processing with the ECMWF fields eliminates forecast errors otherwise present in the NWP data. The finding that winds processed with the NOGAPS forecasts compare more poorly to the truth suggests that the CIMSS quality control shows some sensitivity to forecast errors. However, NWP errors are also clearly not a dominant error source.

The quality control and auto-editing step is an important and complex part of the AMV derivation in the CIMSS processing. It excludes winds based on various consistency checks, and also includes adjustments to the wind speed and possibly the assigned height. The latter is performed as part of the recursive filter analysis and also involves the model background. For the simulated dataset, we found that the main effect of the step is the removal of poorer winds, whereas the adjustments to the wind speed or the assigned pressure were overall relatively small. One exception is mid-tropospheric winds from the infrared channel, for which an average raising of the AMVs by 26 hPa helped to reduce a fast bias versus the true wind field. The findings are in contrast to the monitoring statistics for the AMVs from the NWP Satellite Applications Facility (http://www.metoffice.gov.uk/research/interproj/nwpsaf/satwind_report/index.html). Those statistics indicate considerable differences between raw and auto-edited winds resulting from speed adjustments.

Investigation of a problem area: high-level cirrus clouds

Monitoring of real extra-tropical high-level AMVs (especially in higher wind-speed regimes) typically shows negative speed biases against both other observations and model data. Such biases were also found in the simulated data, and it was therefore decided to investigate these in further detail.

The negative speed bias is commonly attributed to height assignment problems. However, during the course of the present study it was found that height assignment alone

cannot explain all biases found in the simulated dataset. In the following, we will therefore characterise the negative bias only for situations in which height assignment can be ruled out as primary error source, i.e. situations with little vertical wind shear and no multi-layer clouds (with the selection based on the high-resolution ECMWF forecast, i.e. the true atmosphere for our study setup). The limitation to situations in which height assignment should be of lesser importance simplifies our analysis; of course for the general case the height assignment provides an additional source of bias.

Strong negative speed biases in the AMVs are still present in situations with little vertical wind shear and no multi-layer clouds. This can be seen in Figure 3b which shows that for many simulated AMVs the wind speed is considerably lower than the average model speed within the cloud used for tracking. In contrast, the model wind speeds at the assigned heights agree well with the average model speed within the cirrus cloud as indicated in Figure 3a); this is as expected for cases with little wind shear. This confirms that height assignment is a minor error source for the selected cases, as intended by our selection. The main deviations between AMVs and the truth must therefore arise from uncertainties in the tracked speed.

The systematic biases for the selected cases were further characterized as a function of the thickness of the cirrus clouds and its temporal evolution. Such detailed information is readily available in the simulation framework, as the true cloud fields that led to the simulated image sequences are known at their full resolution. Investigations of this kind explore the full potential of the simulation framework.

The investigations showed that the speed bias is stronger for thinner cirrus clouds, whereas thicker cirrus clouds show less bias. This can be seen in Figure 3b, where simulated AMVs derived from thin cirrus clouds (blue and dark green dots) show a particular tendency to have winds speeds lower than their model counterparts. However, simulated AMVs derived from thick cirrus (red dots) are much more symmetrically distributed around the diagonal. A similar analysis showed that clouds exhibiting more temporal evolution within the image-

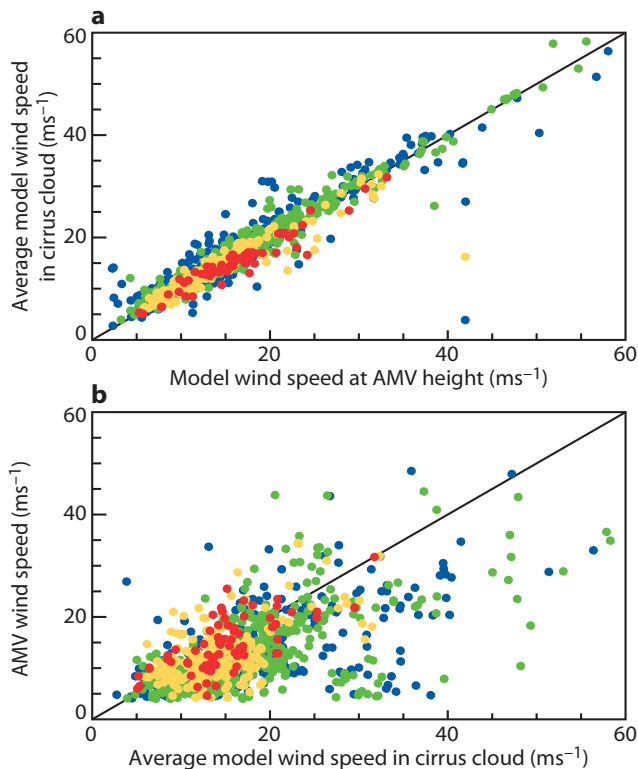


Figure 3 (a) Scatter diagram of the layer-mean model wind speed (ms^{-1}) in the selected cirrus cloud versus the single-level model speed at the originally assigned height for simulated infrared AMVs. See the main text for further details on the selection. (b) Scatter diagram of the speed of the simulated AMV (ms^{-1}) versus the mean model wind speed in the cirrus cloud for the selected cases. For both panels, the colour coding corresponds to the thickness of the cirrus cloud in terms of numbers of model levels. Blue, green, yellow, red is from thin to thick cirrus. These results are based on 'raw' AMVs, i.e. before auto-editing, with Quality Indicator > 60%.

sequence used for the winds derivation also showed larger biases. It is apparent that such situations will pose a challenge to any winds derivation, and it is interesting that the simulation framework can be used to highlight such cases.

Further studies required

The pilot study to use simulations to characterize errors in current AMVs has shown that this method provides a framework with great potential for a better understanding and interpretation of AMVs. The study already provides a number of interesting insights. The interpretation of the results for real AMVs is, however, not straightforward, not least due to the limited study period of 6-hours and the still considerable differences between the nominal model resolution of 10 km and that of today's geostationary imagers (3–5 km). Nevertheless, the study poses some important questions that deserve further attention.

Especially intriguing is the finding that cloud evolution contributes to the bias seen for high-level winds in the simulated dataset. While physically very plausible, this is an aspect that has received much less attention over the years compared to, for instance, the issue of height assignment for AMVs. Height assignment is doubtlessly a crucial issue for AMVs, but the assumption that clouds are passive tracers is equally fundamental in the interpretation of AMVs. Further

studies are needed to determine to what extent clouds can be treated as passive tracers. One possibility would be to use the simulation framework, but to derive AMVs directly from model cloud fields on model or isentropic levels, in order to further simplify the height assignment aspect. A cloud-resolving model may be more suited for this purpose than the global ECMWF model. Another possibility would be to investigate with real AMVs whether situations with thin cirrus clouds and a certain cloud evolution over the tracking period can be linked to stronger biases in the AMVs. If the current findings apply to real data, a quality flag that indicates cloud thickness could prove a useful addition to the AMV product. Further insights are also expected when AMVs can be compared to data from ESA's future ADM-Aeolus wind lidar.

There is clearly scope for further investigations with the simulation framework, and such studies have been recommended by various international bodies, such as the International Winds Working Group. The aspect of interpreting AMVs as layer or horizontal averages rather than single-level point observations could be studied in more detail. This may lead to a reduction in the bias in the interpretation of AMVs. Also, the simulation framework lends itself well to the study of spatial or temporal error correlations in AMVs. Accounting for such error correlations in the assimilation is currently under investigation at ECMWF. At the same time, further work is required to further establish the realism of the simulations and their shortcomings, for example, due to the model resolution, the model cloud parametrization, or the radiative transfer modelling.

It is planned that further simulation studies will be performed in the future, in collaboration with European and American satellite agencies and partners, with the aim of optimizing the processing and interpretation of AMVs and their use in today's assimilation systems.

FURTHER READING

- Forsythe, M., 2008: Third NWP SAF Report (available at http://www.metoffice.gov.uk/research/interproj/nwpsaf/satwind_report/analysis.html)
- Nieman, S.J., W.P. Menzel, C.M. Hayden, D. Gray, S.T. Wanzong, C.S. Velden & J. Daniels, 1997: Fully automated cloud-drift winds in NESDIS operations. *Bull. Am. Meteorol. Soc.*, **78**, 1121–1133.
- Velden, C., J. Daniels, D. Stettner, D. Santek, J. Key, J. Dunion, K. Holmlund, G. Dengel, W. Bresky & P. Menzel, 2005: Recent innovations in deriving tropospheric winds from meteorological satellites. *Bull. Am. Meteorol. Soc.*, **86**, 205–223.
- v. Bremen, L., 2008: Using simulated satellite images to improve the characterisation of Atmospheric Motion Vectors (AMVs) and their errors for Numerical Weather Prediction. *NWP-SAF Visiting Scientist Report NWPSAF-EC-VS-015*, 41 pp., available from <http://www.metoffice.gov.uk/research/interproj/nwpsaf/vs.html>
- Wanzong, S., C.S. Velden, I. Genkova, D.A. Santek, N. Bormann, J. Thépaut, D. Salmond, M. Hortal, J. Li, E.R. Olson & J.A. Otkin, 2007: The use of simulated datasets in atmospheric motion vector research. In *Joint 2007 EUMETSAT Meteorological Satellite Conference and the 15th Satellite Meteorology & Oceanography Conference of the American Meteorological Society*, Amsterdam, The Netherlands, September 2007.

ECMWF Calendar 2010

Jan 11–15	MACC General Assembly	Apr 28–29	Policy Advisory Committee (29 th Session)
Feb 1–5	Training Course – Use and interpretation of ECMWF products	May 25–26	Security Representatives' Meeting
Feb 8–12	Training Course – Use and interpretation of ECMWF products	May 26–28	Computer Representatives' Meeting
Feb 23–Mar 24	Training Course – Use of computing facilities	Jun 9–11	Forecast Products – Users' Meeting
Feb 23–26	GRIB API: library and tools	Jun 15–17	Workshop on 'Assimilating satellite observations of clouds and precipitation into NWP models'
Mar 1–5	Introduction for new users/MARS	Jun 24–25	Council (73 rd Session)
Mar 8–9	MAGICS	Sep 6–9	Seminar on 'Predictability in the European and Atlantic regions from days to years'
Mar 10–12	METVIEW	Oct 4–6	Scientific Advisory Committee (39 th Session)
Mar 15–19	Use of supercomputing resources	Oct 6–8	Technical Advisory Committee (42 nd Session)
Mar 22–24	Introduction to SMS/XCDP	Oct 11–15	Training Course – Use and interpretation of ECMWF products for WMO Members
Apr 12– May 27	Training Course – Numerical Weather Prediction	Oct 11–12	Finance Committee (85 th Session)
Apr 12–16	Numerical methods, adiabatic formulation of models and ocean wave forecasting	Oct 12–13	Policy Advisory Committee (30 th Session)
Apr 19–28	Predictability, diagnostics and seasonal forecasting	Oct 19*	Advisory Committee of Co-operating States (16 th Session)
May 5–14	Data assimilation and use of satellite data	Nov 1–5	14 th Workshop on 'Use of High Performance Computing in Meteorology'
May 17–27	Parametrization of diabatic processes	Nov 8–10	Workshop on 'Non-hydrostatic modelling'
Apr 20–21	Advisory Committee for Data Policy (11 th Session)	Dec 7–8	Council (74 th Session)
Apr 27–28	Finance Committee (84 th Session)		

* To be confirmed

ECMWF publications

(see <http://www.ecmwf.int/publications/>)

Technical Memoranda

- 597 **Vitard, F. & F. Molteni:** Simulation of the MJO and its teleconnections in an ensemble of 46-day EPS hindcasts. *September 2009*
- 596 **Kaiser, J.W., J. Flemming, M.G. Schultz, M. Suttie & M.J. Wooster:** The MACC Global Fire Assimilation System: First emission products (GFASv0). *August 2009*

- 595 **Balmaseda, M.A., L. Ferranti, F. Molteni & T.N. Palmer:** Impact of 2007 and 2008 Arctic ice anomalies on the atmospheric circulation: Implications for long-range predictions. *August 2009*

ERA Report Series

- 1 **Berrisford, P., D. Dee, K. Fielding, M. Fuentes, P. Kallberg, S. Kobayashi & S. Uppala:** The ERA-Interim archive. *August 2009*

Index of past newsletter articles

This is a selection of articles published in the *ECMWF Newsletter* series during the last five years. Articles are arranged in date order within each subject category. Articles can be accessed on the ECMWF public website – www.ecmwf.int/publications/newsletter/index.html

	No.	Date	Page		No.	Date	Page
NEWS							
Co-operation Agreement with Bulgaria	121	Autumn 2009	2	Co-operation Agreement signed with Morocco	110	Winter 2006/07	9
Results of the readership survey	121	Autumn 2009	3	Co-operation Agreement with Estonia	106	Winter 2005/06	8
Operational assimilation of NOAA-19 ATOVS data	121	Autumn 2009	4	Long-term co-operation established with ESA	104	Summer 2005	3
30 years of world class weather forecasts	121	Autumn 2009	6	Co-operation Agreement with Lithuania	103	Spring 2005	24
71 st Council session on 25–26 June	120	Summer 2009	3	Collaboration with the Executive Body of the Convention on Long-Range Transboundary Air Pollution	103	Spring 2005	24
EUMETNET's 'Oslo Declaration'	120	Summer 2009	3	25 years since the first operational forecast	102	Winter 2004/05	36
Operational assimilation of Indian radiosondes	120	Summer 2009	4	COMPUTING			
Assimilation of IASI in NWP	120	Summer 2009	5	ARCHIVING, DATA PROVISION AND VISUALISATION			
Goodbye GEMS – Hello MACC	120	Summer 2009	6	New Automated Tape Library for the Disaster Recovery System	113	Autumn 2007	34
Ocean waves at ECMWF	120	Summer 2009	7	The next generation of ECMWF's meteorological graphics library – Magics++	110	Winter 2006/07	36
ECMWF Annual Report for 2008	120	Summer 2009	7	Computers, Networks, Programming, Systems Facilities and Web			
Forecast Products Users' Meeting, June 2009	120	Summer 2009	8	The EU-funded BRIDGE project	117	Autumn 2008	29
Diagnostics of data assimilation system performance	120	Summer 2009	9	ECMWF's Replacement High Performance Computing Facility 2009–2013	115	Spring 2008	44
Philippe Bougeault leaves ECMWF	119	Spring 2009	3	Improving the Regional Meteorological Data Communications Network (RMDCN)	113	Autumn 2007	36
RMetS recognises the achievements of Adrian Simmons and Tim Palmer	119	Spring 2009	4	New features of the Phase 4 HPC facility	109	Autumn 2006	32
A new Head of Research for ECMWF	119	Spring 2009	4	Developing and validating Grid Technology for the solution of complex meteorological problems	104	Summer 2005	22
ERA-Interim for climate monitoring	119	Spring 2009	5	Migration of ECFS data from TSM to HPSS ("Back-archive")	103	Spring 2005	22
The Call Desk celebrates 15 years of service	119	Spring 2009	6	METEOROLOGY			
ECMWF Seminar on the 'Diagnosis of Forecasting and Data Assimilation Systems'	119	Spring 2009	7	OBSERVATIONS AND ASSIMILATION			
ERA-40 article designated as a 'Current Classic'	119	Spring 2009	7	The new all-sky assimilation system for passive microwave satellite imager observations	121	Autumn 2009	7
Weather forecasting service for the Dronning Maud Land Air Network (DROMLAN)	119	Spring 2009	8	Evaluation of AMVs derived from ECMWF model simulations	121	Autumn 2009	30
ECMWF's plans for 2009	118	Winter 2008/09	2	Solar biases in the TRMM microwave imager (TMI)	119	Spring 2009	18
Use of high performance computing in meteorology	118	Winter 2008/09	5	Variational bias correction in ERA-Interim	119	Spring 2009	21
Atmosphere–Ocean Interaction	118	Winter 2008/09	6	Towards the assimilation of ground-based radar precipitation data in the ECMWF 4D-Var	117	Autumn 2008	13
Use of GIS/OGS standards in meteorology	118	Winter 2008/09	8	Progress in ozone monitoring and assimilation	116	Summer 2008	35
Additional ERA-Interim products available	118	Winter 2008/09	9	Improving the radiative transfer modelling for the assimilation of radiances from SSU and AMSU-A stratospheric channels	116	Summer 2008	43
ECMWF workshops and scientific meetings in 2009	118	Winter 2008/09	10	ECMWF's 4D-Var data assimilation system – the genesis and ten years in operations	115	Spring 2008	8
ECMWF Education and Training Programme 2009	117	Autumn 2008	2	Towards a climate data assimilation system: status update of ERA-Interim	115	Spring 2008	12
GRAS SAF Workshop on applications of GPS radio occultation measurements	117	Autumn 2008	4	Operational assimilation of surface wind data from the Metop ASCAT scatterometer at ECMWF	113	Autumn 2007	6
PREVIEW Data Targeting System (DTS)	117	Autumn 2008	5	Evaluation of the impact of the space component of the Global Observing System through Observing System Experiments	113	Autumn 2007	16
Verification of severe weather forecasts	117	Autumn 2008	6	Data assimilation in the polar regions	112	Summer 2007	10
GMES Forum, 16–17 September 2008	117	Autumn 2008	7	Operational assimilation of GPS radio occultation measurements at ECMWF	111	Spring 2007	6
Exploratory analysis and verification of seasonal forecasts with the KNMI Climate Explorer	116	Summer 2008	4				
Optimisation and improvements to scalability of 4D-Var for Cy33r2	116	Summer 2008	6				
Operational assimilation of GRAS measurements at ECMWF	116	Summer 2008	7				
First meeting of the TAC Subgroup on the RMDCN	115	Spring 2008	2				
Signing of the Co-operation Agreement between ECMWF and Latvia	115	Spring 2008	4				
Two new Co-operation Agreements	114	Winter 2007/08	4				
Signing of the Co-operation Agreement between ECMWF and Montenegro	114	Winter 2007/08	7				
New High Performance Computing Facility	114	Winter 2007/08	13				
Fifteenth anniversary of EPS	114	Winter 2007/08	14				

	No.	Date	Page		No.	Date	Page
OBSERVATIONS AND ASSIMILATION				ENSEMBLE PREDICTION AND SEASONAL FORECASTING			
The value of targeted observations	111	Spring 2007	11	Comparing and combining deterministic and ensemble forecasts: How to predict rainfall occurrence better	106	Winter 2005/06	17
Assimilation of cloud and rain observations from space	110	Winter 2006/07	12	EPS skill improvements between 1994 and 2005	104	Summer 2005	10
ERA-Interim: New ECMWF reanalysis products from 1989 onwards	110	Winter 2006/07	25	Ensembles-based predictions of climate change and their impacts (ENSEMBLES Project)	103	Spring 2005	16
Analysis and forecast impact of humidity observations	109	Autumn 2006	11	OCEAN AND WAVE MODELLING			
Surface pressure bias correction in data assimilation	108	Summer 2006	20	NEMOVAR: A variational data assimilation system for the NEMO ocean model	120	Summer 2009	17
A variational approach to satellite bias correction	107	Spring 2006	18	Climate variability from the new System 3 ocean reanalysis	113	Autumn 2007	8
“Wavelet” Jb – A new way to model the statistics of background errors	106	Winter 2005/06	23	Progress in wave forecasts at ECMWF	106	Winter 2005/06	28
New observations in the ECMWF assimilation system: satellite limb measurements	105	Autumn 2005	13	Ocean analysis at ECMWF: From real-time ocean initial conditions to historical ocean analysis	105	Autumn 2005	24
The direct assimilation of cloud-affected infrared radiances in the ECMWF 4D-Var	120	Summer 2009	32	High-precision gravimetry and ECMWF forcing for ocean tide models	105	Autumn 2005	6
CO ₂ from space: estimating atmospheric CO ₂ within the ECMWF data assimilation system	104	Summer 2005	14	ENVIRONMENTAL MONITORING			
Sea ice analyses for the Baltic Sea	103	Spring 2005	6	Smoke in the air	119	Spring 2009	9
The ADM-Aeolus satellite to measure wind profiles from space	103	Spring 2005	11	GEMS aerosol analyses with the ECMWF Integrated Forecast System	116	Summer 2008	20
Atlas describing the ERA-40 climate during 1979–2001	103	Spring 2005	20	Progress with the GEMS project	107	Spring 2006	5
FORECAST MODEL				A preliminary survey of ERA-40 users developing applications of relevance to GEO (Group on Earth Observations)	104	Summer 2005	5
Improvements in the stratosphere and mesosphere of the IFS	120	Summer 2009	22	The GEMS project – making a contribution to the environmental monitoring mission of ECMWF	103	Spring 2005	17
Parametrization of convective gusts	119	Spring 2009	15	METEOROLOGICAL APPLICATIONS AND STUDIES			
Towards a forecast of aerosols with the ECMWF Integrated Forecast System	114	Winter 2007/08	15	Tracking fronts and extra-tropical cyclones	121	Autumn 2009	9
A new partitioning approach for ECMWF's Integrated Forecast System	114	Winter 2007/08	17	Progress in implementing Hydrological Ensemble Prediction Systems (HEPS) in Europe for operational flood forecasting	121	Autumn 2009	20
Advances in simulating atmospheric variability with IFS cycle 32r3	114	Winter 2007/08	29	EPS/EFAS probabilistic flood prediction for Northern Italy: the case of 30 April 2009	120	Summer 2009	10
A new radiation package: McRad	112	Summer 2007	22	Use of ECMWF lateral boundary conditions and surface assimilation for the operational ALADIN model in Hungary	119	Spring 2009	29
Ice supersaturation in ECMWF's Integrated Forecast System	109	Autumn 2006	26	Using ECMWF products in global marine drift forecasting services	118	Winter 2008/09	16
Towards a global meso-scale model: The high-resolution system T799L91 and T399L62 EPS	108	Summer 2006	6	Record-setting performance of the ECMWF IFS in medium-range tropical cyclone track prediction	118	Winter 2008/09	20
The local and global impact of the recent change in model aerosol climatology	105	Autumn 2005	17	The ECMWF ‘Diagnostic Explorer’: A web tool to aid forecast system assessment and development	117	Autumn 2008	21
Improved prediction of boundary layer clouds	104	Summer 2005	18	Diagnosing forecast error using relaxation experiments	116	Summer 2008	24
ENSEMBLE PREDICTION AND SEASONAL FORECASTING				ECMWF's contribution to AMMA	115	Spring 2008	19
An experiment with the 46-day Ensemble Prediction System	121	Autumn 2009	25	Coupled ocean-atmosphere medium-range forecasts: the MERSEA experience	115	Spring 2008	27
EUROSIP: multi-model seasonal forecasting	118	Winter 2008/09	10	Probability forecasts for water levels in The Netherlands	114	Winter 2007/08	23
Using the ECMWF reforecast dataset to calibrate EPS forecasts	117	Autumn 2008	8	Impact of airborne Doppler lidar observations on ECMWF forecasts	113	Autumn 2007	28
The THORPEX Interactive Grand Global Ensemble (TIGGE): concept and objectives	116	Summer 2008	9	Ensemble streamflow forecasts over France	111	Spring 2007	21
Implementation of TIGGE Phase 1	116	Summer 2008	10	Hindcasts of historic storms with the DWD models GME, LMQ and LMK using ERA-40 reanalyses	109	Autumn 2006	16
Predictability studies using TIGGE data	116	Summer 2008	16	Hurricane Jim over New Caledonia: a remarkable numerical prediction of its genesis and track	109	Autumn 2006	21
Merging VarEPS with the monthly forecasting system: a first step towards seamless prediction	115	Spring 2008	35	Recent developments in extreme weather forecasting	107	Spring 2006	8
Seasonal forecasting of tropical storm frequency	112	Summer 2007	16	MERSEA – a project to develop ocean and marine applications	103	Spring 2005	21
New web products for the ECMWF Seasonal Forecast System-3	111	Spring 2007	28				
Seasonal Forecast System 3	110	Winter 2006/07	19				
The ECMWF Variable Resolution Ensemble Prediction System (VAREPS)	108	Summer 2006	14				
Limited area ensemble forecasting in Norway using targeted EPS	107	Spring 2006	23				
Ensemble prediction: A pedagogical perspective	106	Winter 2005/06	10				

Useful names and telephone numbers within ECMWF

Telephone

Telephone number of an individual at the Centre is:
 International: +44 118 949 9 + three digit extension
 UK: (0118) 949 9 + three digit extension
 Internal: 2 + three digit extension
 e.g. the Director's number is:
 +44 118 949 9001 (international),
 (0118) 949 9001 (UK) and 2001 (internal).

E-mail

The e-mail address of an individual at the Centre is:
 firstinitial.lastname@ecmwf.int
 e.g. the Director's address is: D.Marbouty@ecmwf.int
 For double-barrelled names use a hyphen
 e.g. J-N.Name-Name@ecmwf.int

Internet web site

ECMWF's public web site is: <http://www.ecmwf.int>

	Ext		Ext
Director		Meteorological Division	
Dominique Marbouty	001	<i>Division Head</i>	
Deputy Director & Head of Operations Department		Erik Andersson	060
Walter Zwiefelhofer	003	<i>Meteorological Applications Section Head</i>	
Head of Research Department		Alfred Hofstadler	400
Erland Källén	003	<i>Data and Services Section Head</i>	
Head of Administration Department		Baudouin Raoult	404
Ute Dahremöller	007	<i>Graphics Section Head</i>	
		Stephan Siemen	375
Switchboard		<i>Meteorological Operations Section Head</i>	
ECMWF switchboard	000	David Richardson	420
Advisory		<i>Meteorological Analysts</i>	
Internet mail addressed to Advisory@ecmwf.int		Antonio Garcia-Mendez	424
Telefax (+44 118 986 9450, marked User Support)		Anna Ghelli	425
Computer Division		Claude Gibert (web products)	111
<i>Division Head</i>		Fernando Prates	421
Isabella Weger	050	Meteorological Operations Room	426
<i>Computer Operations Section Head</i>		Data Division	
Sylvia Baylis	301	<i>Division Head</i>	
<i>Networking and Computer Security Section Head</i>		Jean-Noël Thépaut	030
Rémy Giraud	356	<i>Data Assimilation Section Head</i>	
<i>Servers and Desktops Section Head</i>		Lars Isaksen	852
Richard Fisker	355	<i>Satellite Data Section Head</i>	
<i>Systems Software Section Head</i>		Peter Bauer	080
Neil Storer	353	<i>Re-Analysis Section Head</i>	
<i>User Support Section Head</i>		Dick Dee	352
Umberto Modigliani	382	Probabilistic Forecasting & Diagnostics Division	
<i>User Support Staff</i>		<i>Division Head</i>	
Paul Dando	381	Tim Palmer	600
Dominique Lucas	386	<i>Seasonal Forecasting Section Head</i>	
Carsten Maaß	389	Franco Molteni	108
Pam Prior	384	Model Division	
Christian Weihrauch	380	<i>Division Head</i>	
Computer Operations		Martin Miller	070
<i>Call Desk</i>		<i>Numerical Aspects Section Head</i>	
<i>Call Desk email:</i> calldesk@ecmwf.int		Agathe Untch	704
<i>Console – Shift Leaders</i>		<i>Physical Aspects Section Head</i>	
<i>Console fax number</i> +44 118 949 9840		Anton Beljaars	035
<i>Console email:</i> newops@ecmwf.int		<i>Ocean Waves Section Head</i>	
<i>Fault reporting – Call Desk</i>		Peter Janssen	116
<i>Registration – Call Desk</i>		GMES Coordinator	
<i>Service queries – Call Desk</i>		Adrian Simmons	700
<i>Tape Requests – Tape Librarian</i>		Education & Training	
		Renate Hagedorn	257
		ECMWF library & documentation distribution	
		Els Kooij-Connally	751